Development of Pediatric Patient-Derived Extracellular Matrix-Incorporated Gelatin-Based Hydrogels for Cardiac Tissue Engineering

by

Yuka Sugamura

A Thesis Presented in Partial Fulfillment
of the Requirements for the Degree
Master of Science

Approved October 2018 by the
Graduate Supervisory Committee:

Mehdi Nikkhah, Chair
Barbara Smith
Brigham Willis

ARIZONA STATE UNIVERSITY

December 2018

ABSTRACT

Severe cases of congenital heart defect (CHD) require surgeries to fix the structural problem, in which artificial grafts are often used. Although outcome of surgeries has improved over the past decades, there remains to be patients who require re-operations due to graft-related complications and the growth of patients which results in a mismatch in size between the patient's anatomy and the implanted graft. A graft in which cells of the patient could infiltrate, facilitating transformation of the graft to a native-like tissue, and allow the graft to grow with the patient heart would be ideal. Cardiac tissue engineering (CTE) technologies, including extracellular matrix (ECM)-based hydrogels has emerged as a promising approach for the repair of cardiac damage. However, most of the previous studies have mainly focused on treatments for ischemic heart disease and related heart failure in adults, therefore the potential of CTE for CHD treatment is underexplored. In this study, a hybrid hydrogel was developed by combining the ECM derived from cardiac tissue of pediatric CHD patients and gelatin methacrylate (GelMA). In addition, the influence of incorporating gold nanorods (GNRs) within the hybrid hydrogels was studied. The functionalities of the ECM-GelMA-GNR hydrogels as a CTE scaffold were assessed by culturing neonatal rat cardiomyocytes on the hydrogel. After 8 days of cell culture, highly organized sarcomeric α-actinin structures and connexin 43 expression were evident in ECM- and GNR-incorporated hydrogels compared to pristine GelMA hydrogel, indicating cell maturation and formation of cardiac tissue. The findings of this study indicate the promising potential of ECM-GelMA-GNR hybrid hydrogels as a CTE approach for CHD treatment.

As another approach to improve CHD treatment, this study sought the possibility of performing a proteomic analysis on cardiac ECM of pediatric CHD patient tissue. As the ECM play important roles in regulating cell signaling, there is

an increasing interest in studying the ECM proteome and the influences caused by diseases. Proteomics on ECM is challenging due to the insoluble nature of ECM proteins which makes protein extraction and digestion difficult. In this study, as a first step to perform proteomics, optimization on sample preparation procedure was attempted.

DEDICATION

I dedicate my work to my parents, Mr. & Mrs. Sugamura.

ACKNOWLEDGMENTS

First, I would like to express my sincere gratitude to my committee chair, Dr. Mehdi Nikkhah, for allowing me to conduct this research under his auspices. I am grateful for the freedom he gave me to do this work, which allowed me to learn a lot as a researcher. I also appreciate his guidance and support which helped me complete my master's thesis in a timely manner.

I would also like to thank my committee members, Dr. Barbara Smith and Dr. Brigham Willis, for their support and encouragement which helped me during the difficult times.

Additionally, I would like to express my heartfelt thanks to Dr. Ali Navaei for teaching me laboratory techniques from the basics as well as helping me with my experiments, and Ms. Harpinder Saini for providing me all possible help and support throughout my research work. I would also like to thank all the members of the lab for their support.

I would like to thank the members of Arizona State University OKED Mass Spectrometry Core Facility, Dr. Jia Fan, Ms. Jennifer Esman, Dr. Megan Maurer, and Mr. Jason Steel for carrying out the MALDI experiment as well as for their support. I would also like to thank Dr. Qingbo Shu, Ms. Crystal Willingham, and Ms. Briana Martinez, for providing many great advices and guidance without which I would not have been able to carry out the experiments related to proteomics and decellularization.

In addition, I would also like to thank my academic advisor Ms. Laura Hawes, for her guidance and support throughout my master's degree program.
Lastly, I would like to acknowledge Phoenix Children's Hospital for their cooperation and funding for this project.

TABLE OF CONTENTS

LIST OF FIGURES

LIST OF ABBREVIATIONS

$AgNO_3$	Silver nitrate
AHA	American Heart Association
BMC	Bone marrow cells
BSA	Bovine serum albumin
CHD	Congenital heart defect
CNBr	Cyanogen bromide
CT	Computed tomography
CTE	Cardiac tissue engineering
CTAB	Hexadecyltrimethylammonium bromide
DAPI	4', 6-diamidino-2-phenylindole
DMEM	Dulbecco’s modified eagle medium
DNase	Deoxyribonuclease
DPBS	Dulbecco's phosphate buffered saline
dsDNA	Double-stranded DNA
DW	Distilled water
ECM	Extracellular matrix
EDTA	Ethylenediaminetetraacetic acid
FASP	Filter-aided sample preparation
FBS	Fetal bovine serum
FDA	Food and Drug Administration
GAG	Glycosaminoglycan
GelMA	Gelatin methacrylate
GNR	Gold nanorod
HBSS	Hank’s balanced salt solution
HCl	Hydrochloric acid

$HAuCl_4$	Hydrogen tetrachloroaurate
HLHS	Hypoplastic left heart syndrome
IVC	Inferior vena cava
MALDI	Matrix assisted laser desorption/ionization
MCP-1	Monocyte chemotactic protein-1
MI	Myocardial infarction
$NaBH_4$	Sodium borohydride
NaOH	Sodium hydroxide
PBS	Phosphate buffered saline
PCH	Phoenix Children's Hospital
PCLA	Poly(ε-caprolactone-co-L-lactide)
PEUU	Polyester urethane
PGA	Polyglycolic acid
P(GA/CL)	Glycolide and ε-caprolactone copolymer
PHB	Polyhydroxybutyrate
PIPAAm	Poly(N-isopropyllacrylamide)
PLA	Polylactic acid
PLLA	Poly-L-lactide acid
PTFE	Polytetrafluoroethylene
RNase	Ribonuclease
RV	Right ventricular
RVOT	Right ventricular outflow tract
SD	Standard deviation
SDS	Sodium dodecyl sulfate
SIS-ECM	Small intestine submucosa extracellular matrix
TCEP	Tris(2-carboxyethyl)phosphine

TEAB	Triethylammonium bicarbonate
TEVG	Tissue-engineered vascular graft
TFA	Trifluoroacetic acid
TOF	Tetralogy of Fallot
Tris-HCl	Tris(hydroxymethyl)aminomethane-hydrochloride
TMSPMA	3-(trimethoxysilyl) propyl methacrylate
VSD	Ventricular septal defect

CHAPTER 1

INTRODUCTION

1.1 Extracellular matrix

1.1.1 Overview

Extracellular matrix (ECM) consists of a complex meshwork of highly cross-linked proteins and polysaccharides which exists as interstitial forms within the tissue and as specialized forms such as basement membranes (Naba et al. 2012). According to the report from Naba et al., who characterized the ECM of murine lung and colon, the "matrisome" which is defined as the ensemble of ECM proteins and associated factors, comprise over 100 ECM proteins (Naba et al. 2012). The mesh-like structure is formed by core ECM components which involve fibrotic proteins (e.g. collagen type I, elastin) and other glycoproteins (e.g. laminin) and proteoglycans (Naba et al. 2012). In addition, there is a group of ECM components that could be categorized as ECM-affiliated proteins, which refers to proteins that share either some architectural or biochemical similarities with the ECM proteins (e. g. ficolins, mucins) or that are known to be associated with ECM proteins (Naba et al. 2012). Cells interact with the ECM components via transmembrane receptors, and this cell-matrix interaction stimulate various signaling pathways that are responsible for cell functions including proliferation, survival, and differentiation (Naba et al. 2012). The tissue-dependent composition and topology, as well as biophysical properties (deformability or stiffness) dictates cell responses (Franz, Stewart, and Weaver 2010 and Schwartz 2010). Furthermore, the ECM has a heterogeneous, highly dynamic structure that is constantly being remodeled, either enzymatically or non-enzymatically, and its molecular components are subjected to numerous post-translational modifications (Franz, Stewart, and Weaver 2010). This complexity allows the ECM to provide the right cues to the cells. Along with its

structural role, ECM is also responsible for the buffering actions that maintain homeostasis and water retention of the ECM (Franz, Stewart, and Weaver 2010). Moreover, it serves as a reservoir of growth factors, cytokines, and ECM-remodeling enzymes which collaborate with ECM proteins and cell-surface receptors to modulate cell signaling (Naba et al. 2012).

The interaction between the ECM and cells is mainly mediated by integrins, a transmembrane heterodimer. Integrins serve as a link between the cytoskeleton and ECM components (Alberts et al. 2002 and Danen n.d.) allowing cells to convert the mechanical signals to biochemical signals (Geiger et al. 2001). This integrin-mediated interaction modulates signaling cascades which are responsible for important cellular processes including cell motility, survival, proliferation, and differentiation (Danen n.d.).

1.1.2 Components of the ECM

Collagen is known to be the most abundant protein within the ECM (Yue 2014). 28 types of collagens have been identified in vertebrates (Gordon and Hahn 2010), all of which have the basic structure of triple helix (Mouw, Ou, and Weaver 2014). Collagen triple helix serves as a motif to which various proteins, including cell surface receptors and glycosaminoglycans (GAGs), could bind (Mouw, Ou, and Weaver 2014). Collagen types I and III is the primary component of cardiac interstitial collagen (Villarreal and Kim 1998) and serve as a backbone of ECM. These types form fibrils where collagen molecules are packed together in a side-by-side manner by formation of covalent cross-links between the lysine residues of two collagen chains. This interaction stabilizes the side-by-side structure and contribute to the tensile strength of collagen fibers (Lodish et al. 2000).

Elastin is another fibrotic protein in the ECM, which is the main component of elastic fibers. Elastic fibers are a network found in the ECM of tissues which requires

strength and elasticity, such as blood vessels. Elastin is a highly hydrophobic protein which are formed by intensive crosslinking of tropoelastin into the form of network of fibers and sheets. The elastin core is surrounded by a sheath of microfibrils made of glycoproteins, such as fibrillin (Alberts et al. 2002).

Fibronectin are also found as fibrils in the ECM. Formation of fibronectin fibrils takes place on the surface of specific cells (e.g. fibroblasts) (Alberts et al. 2002). The resulting fibrils are highly insoluble due to disulfide bonds formed between fibronectin dimers (Alberts et al. 2002). Fibronectin and intracellular actin filaments interact via integrins, which interaction is responsible for assembly of fibrils as well as cell adhesion (Alberts et al. 2002). Furthermore, it has been demonstrated that fibronectin is an essential component of heart development. Lack of fibronectin during development results in abnormalities in blood vessel formation, which is thought to be due to alteration in cell-ECM interactions (Alberts et al. 2002).

Collagen type IV and laminin forms the reticulum of the basal lamina, a sheet-like structure on which most epithelial and endothelial cells reside on. Both have binding sites for a vast range of macromolecules, including proteoglycans and cell surface receptors (Lodish et al. 2002). Entactin, a basal lamina protein, facilitates the assembly of the basal lamina by linking the laminin and collagen type IV. Entactin can also bind to fibronectin (Chung and Durkin 1990).

In addition to the insoluble components of ECM described above, the ECM contains soluble components, such as proteoglycans. Proteoglycans consist of a core protein and one or more covalently attached GAGs, which are linear polysaccharides. Due to the high content of charged polysaccharides, proteoglycans are highly hydrated. This property contributes to the role of ECM to maintain its volume and water content, as well as to facilitate diffusion of small molecules between cells and tissues (Lodish et al. 2002 and Alberts et al. 2002). In addition, proteoglycans can

bind to various bioactive molecules including ECM-affiliated proteins, ECM regulators, and secreted factors, and thought to be contributing to regulation of cell activities (Alberts et al. 2002). The binding between proteoglycans and bioactive molecules can control the range and duration of activity of the bioactive molecules, as the molecules can be immobilized to be effective in a specific region, released in a controlled manner, and could be protected from proteolytic degradation (Alberts et al. 2002). Furthermore, proteoglycans can control the activity of proteins by either steric blocking or by alteration of the presentation to cell-surface receptors (Alberts et al. 2002). Perlecan is a type of heparan sulfate proteoglycan. By its modular structure, it takes part in a wide range of cellular processes including adhesion, proliferation, modulation of growth factor signaling, autophagy, cardiovascular development, inflammation and wound healing (Gubbiotti, Neill, and Iozzo 2017, Jung et al. 2013, Lord et al. 2014, and Zoeller et al. 2008).

As described above, the ECM involves an intricate and dynamic orchestration of a vast range of macromolecules. This complexity allows the interaction between the ECM and cells to initiate the right cues for cell signaling and dictates cell activity and tissue functions.

1.2 ECM-inspired tissue engineering approaches

Recent research has revealed the importance of ECM not only as a structure for cells to reside, but also as a regulator of cell signaling, guiding them to function in an organized tissue-specific manner. In this regard, the ECM has a high potential as a material for tissue engineering.

Several types of studies have attempted to mimic the structure and functions of ECM using synthetic materials. The approaches to reproduce the architecture of ECM include utilization of micro- and nanofibrillar synthetic biomaterial (Oberpenning et al. 1999), in situ formation of nanofibrillar structures using supramolecular self-

assembly (Kisiday et al. 2002), and micropatterning (Cio et al. 2017). Mann et al. employed a different approach where they attempted to mimic the proteolytic recognition of natural ECMs by incorporating proteolytically degradable domains in synthetic polymer gels (Mann et al. 2001). This approach is based on the knowledge that degradation of ECM components stimulates ECM-cell interaction and cell signaling (Lutolf and Hubbell 2005). As another approach to mimic a different aspect of ECM, i.e. a reservoir of growth factors, biomaterials with features of controlled delivery (Chen and Mooney 2003) or sequential delivery (Zisch et al. 2003) of growth factors have been developed. Lastly, techniques to immobilize active ligands to a polymer material can also be utilized to create an ECM-like scaffold. (Lutolf and Hubbell 2005). This approach has been employed in multiple studies which aimed to understand the mechanism of cell-ECM interaction (Irvine et al. 2002 and Brandley and Schnaar 1989). The abovementioned approaches succeed in mimicking some aspects of the ECM and controlling relatively simple cellular processes. However, compared to the intricate and dynamic nature of the natural ECMs, where complex temporal and spatial coordination of many different cell-matrix and cell-cell interactions take place, they are still oversimplified mimics (Lutolf and Hubbell 2005). Therefore, further research is awaited to control more complicated cell signaling processes simultaneously and sequentially in order to mimic the complexity of ECM.

1.3 Utilization of ECM derived from biological sources

Given the complexity and incomplete understanding in the nature of the ECM, fabrication of an ECM scaffold that fully mimics the biochemistry and architecture of natural ECM is currently not possible (Hussey, Dziki, and Badylak 2018). Alternatively, an approach to derive ECM from tissues via decellularization can allow restoration of tissue-specific microarchitecture and molecular composition (Hussey,

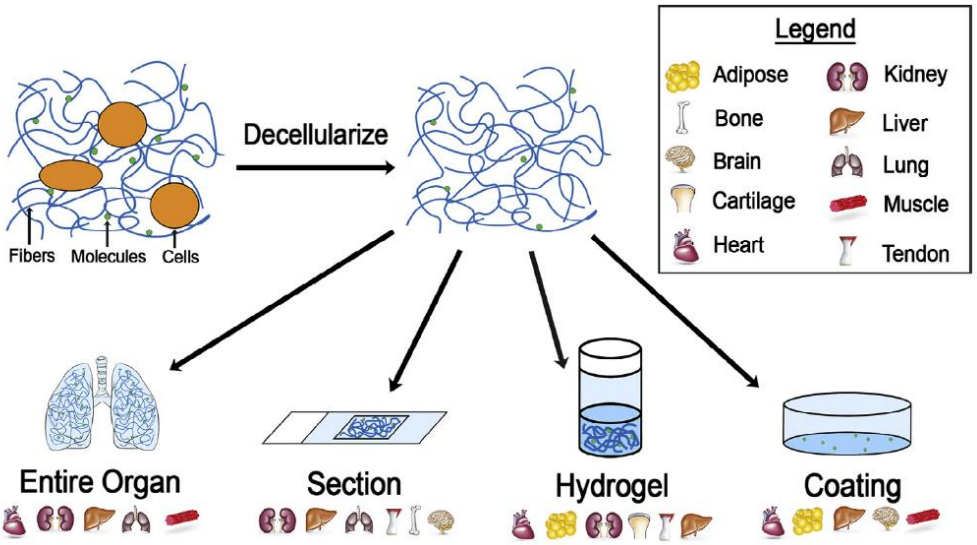

Figure 1 Decellularized tissue materials made from various tissues. After removing the cellular contents of the native tissue, the extracellular matrix remains and can be left unprocessed as an entire organ, or be processed into a section, hydrogel, or coating. The tissues that have been processed for the purpose of testing cell differentiation effects are shown below each material category. Adapted from (Agmon and Christman 2016) with permission from ELSEVIER.

Dziki, and Badylak 2018). In addition, the derived ECM can be used in various forms, which could be another reason for this approach to be utilized in various studies (**Figure 1**). As mentioned later in detail, the small intestine submucosa ECM (SIS-ECM) is now used in cardiac surgery including corrective surgery for CHD. Given that the ECM has a tissue-specific composition which could affect cell-matrix interactions, it would be reasonable to argue that cardiac ECM could potentially be advantageous for cardiac tissue regeneration. Zhang and colleagues, in their *in vitro* study using skin, muscle, and liver cells, reported improved cell adhesion, growth rate, and phenotype when tissue-specific ECM solutions were used to coat cell culture dishes (Zhang et al. 2009).

Cardiac ECM have been utilized mostly in the form of injectable hydrogels which aim to repair cardiac damages caused by ischemic heart diseases. Injectable ECM

hydrogels could be obtained by either enzymatic digestion or homogenization of ECM. The hydrogel can be injected solely or as a carrier to deliver cells.

Extensive study on injectable ECM hydrogels has been carried out by Christman laboratory (Johnson et al. 2014 and 2016, Seif-Naraghi et al. 2013, Singelyn et al. 2009 and 2012, Wassenaar et al. 2016a and 2016b). They have optimized the protocol to decellularize porcine and human cardiac tissue, where the tissue is decellularized using sodium dodecyl sulfate (SDS) and then digestion using pepsin (Johnson et al. 2014 and 2016). The obtained myocardial ECM retained protein components including structural proteins and glycosaminoglycans (Johnson et al. 2014 and Singelyn et al. 2009) and had the ability to self-assemble into a nanofibrous structure at 37 °C. Infiltration of endothelial cells and smooth muscle cells was observed in *in vitro* and *in vivo* studies (Singelyn et al. 2009). Injection of porcine-derived ECM hydrogel to rat hearts which underwent ischemia and reperfusion, resulted in increased recruitment of endogenous cardiomyocytes in the infarcted area (Singelyn et al. 2012). Furthermore, to confirm the safety of the ECM hydrogel, they evaluated the biocompatibility of the material using a rat model. In the healthy rats which received intramyocardial injections of ECM hydrogels, no signs of chronic inflammation were found, which indicate the biocompatible nature of the hydrogel. Hemocompatibility study using human blood also gave positive results as no effect on clotting times or platelet activation was observed (Seif-Naraghi et al. 2013). In addition to the above studies, they have carried out studies to understand the underlying mechanism of tissue regeneration which occur in the ECM hydrogels (Wassenaar et al. 2016b), as well as studies on approaches to modulate the mechanical properties of the ECM hydrogel (Wassenaar et al. 2016a and Johnson et al. 2011).

In line with the results reported by Christman laboratory, Dai et al. reported encouraging results on the potential of injectable ECM hydrogels to repair cardiac damage caused by myocardial infarction (MI). Cardiac ECM hydrogels were injected to the infarcted area 1 week after MI was induced. Assessment carried out at 6 months after injection revealed higher left ventricular (LV) ejection fraction and increased thickness of infarcted LV wall, as well as reduction in extent of LV systolic bulging in the ECM-treated group compared to saline-treated group. The findings indicate the promising potential of the ECM in cardiac function restoration of the infarcted area (Dai et al. 2013).

1.4 Congenital heart defect

Congenital heart defect (CHD) refers to structural problems due to abnormal formation of the heart or major blood vessels. At least 18 distinct types of CHD are known, with many additional anatomic variations (American Heart Association (AHA) n.d.). Examples of defects include holes in the septal (e.g. atrial septal defect, ventricular septal defect (VSD), atrioventricular septal defect) and aorta (e.g. patent ductus arteriosis), abnormalities in vessel connection (e.g. total anomalous pulmonary venous connection, transposition of the great arteries), narrowing of major arteries (e.g. coarctation of the aorta), problems in valve function (e.g. pulmonary valve stenosis, aortic valve stenosis, Ebstein's anomaly, tricuspid atresia, pulmonary atresia), and underdevelopment of chambers (e.g. hypoplastic left heart syndrome (HLHS)) (AHA n. d.) (**Figure 2**). Severity can range from simple defects that could be treated with non-surgical approaches, to complex structural problems such as Tetralogy of Fallot (TOF: a combination of four heart defects) and HLHS, where surgical correction is necessary (AHA n.d.). Approximately 1% of new born babies are diagnosed as CHD, including 25% of severe CHDs who requires surgical interventions (Botto, Correa, and Erickson 2001). Surgeries often use artificial grafts

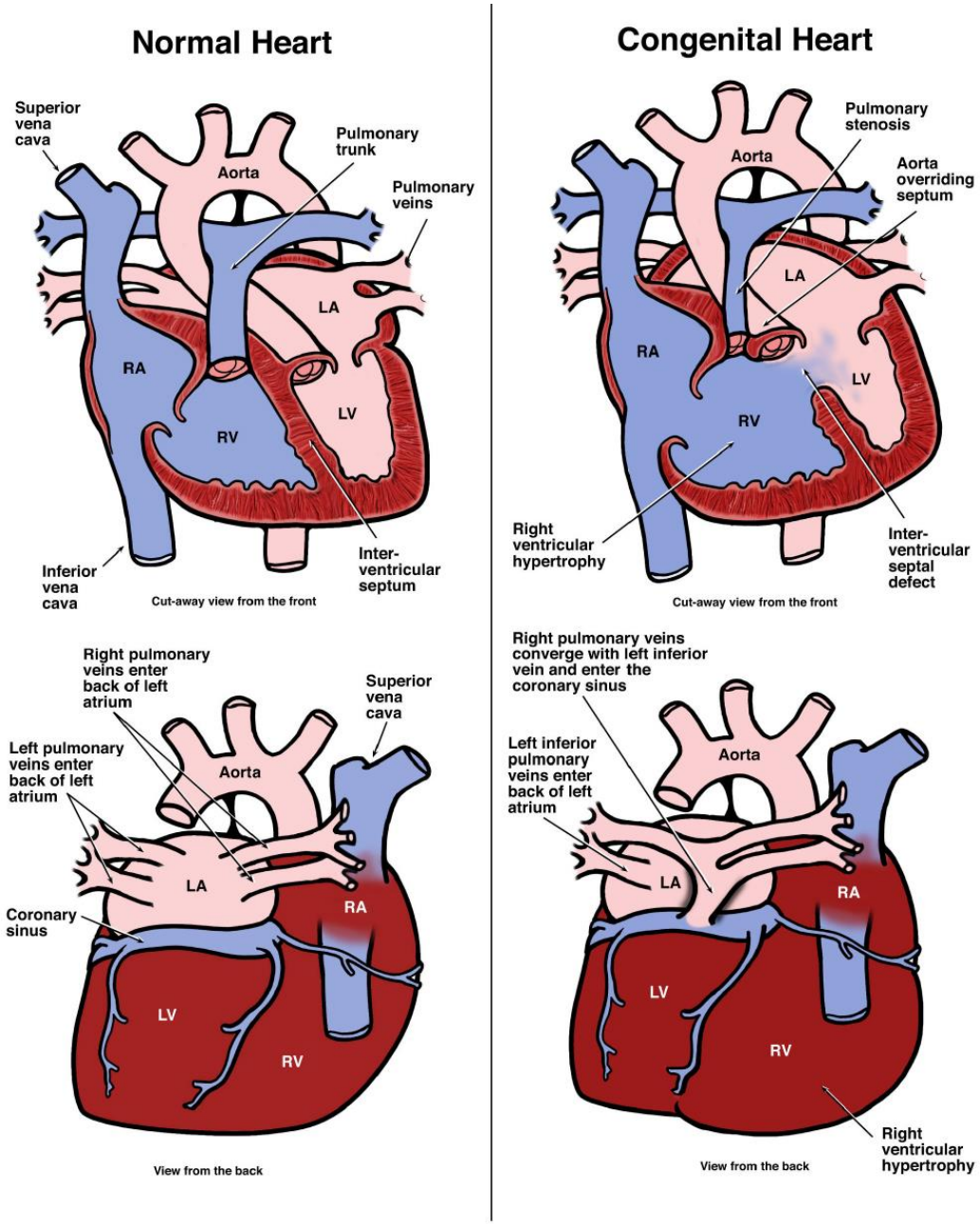

Figure 2 Congenital heart abnormalities in the new born. Adapted from (Nucleus Medical Media 2015) with permission.

to fix the defect. Thanks to the advance in medicine and surgical techniques, outcomes of surgical interventions for CHD have improved dramatically over the past decades (Castañeda, 2005). However, there remains patients who require multiple re-interventions throughout their lifetime because of graft-related complications

including degeneration and calcification, and the growth of patients resulting in a mismatch in size between the patient's anatomy and the implanted graft. (Witt et al. 2013, and Holst et al. 2018). As repeated operations incur additive risks (Holst et al. 2018) and causes burden and pain to the patient, minimizing the number of re-interventions could be an effective approach to improve outcome of CHD treatment.

Surgical procedures, although they may differ depending on the type of defect and the patient's condition, could involve the following types of procedures to correct abnormalities in blood circulation; closure of holes by stitching or using a patch, enlargement or bypassing of narrowed vessels, cutting and reconnecting vessels, and replacement or repair of heart valves (MedlinePlus n.d.). These surgical procedures often require additional substances to "patch" the heart. Autologous pericardium can be used, however, the amount of tissue that could be harvested is limited. In cases where a large substance is necessary, synthetic materials such as Dacron (polyethylene terephthalate) and Gore-tex (polytetrafluoroethylene: PTFE) or bovine pericardium are often used (Kimura 2018 and MedlinePlus n.d.). Although the outcomes of surgeries using these materials are now good, a common critical limitation of these materials is the lack of capacity to grow (Kimura 2018). Growth is an important factor that should be considered in CHD treatment, as growth from infant to adult involve significant changes in size of the anatomical structures. There is an unmet need for a graft which could grow with the patient after implantation (Kimura 2018), as it can potentially avoid re-interventions due to size discrepancy between the patient's anatomy and the implanted graft when the patient grows up.

1.5 Tissue engineering approaches for CHD treatment

Cardiac tissue engineering (CTE) techniques has the potential to address the need of grafts with desirable features including architecture, material composition and growth potential. Tissue engineering approaches which have potential for CHD

treatment include; (1) scaffold-based approaches, (2) scaffold-free approaches, (3) decellularization-recellularization (Zimmermann and Cesnjevar 2009) (**Figure 3**), and (4) biotubes (Kato et al. 2016).

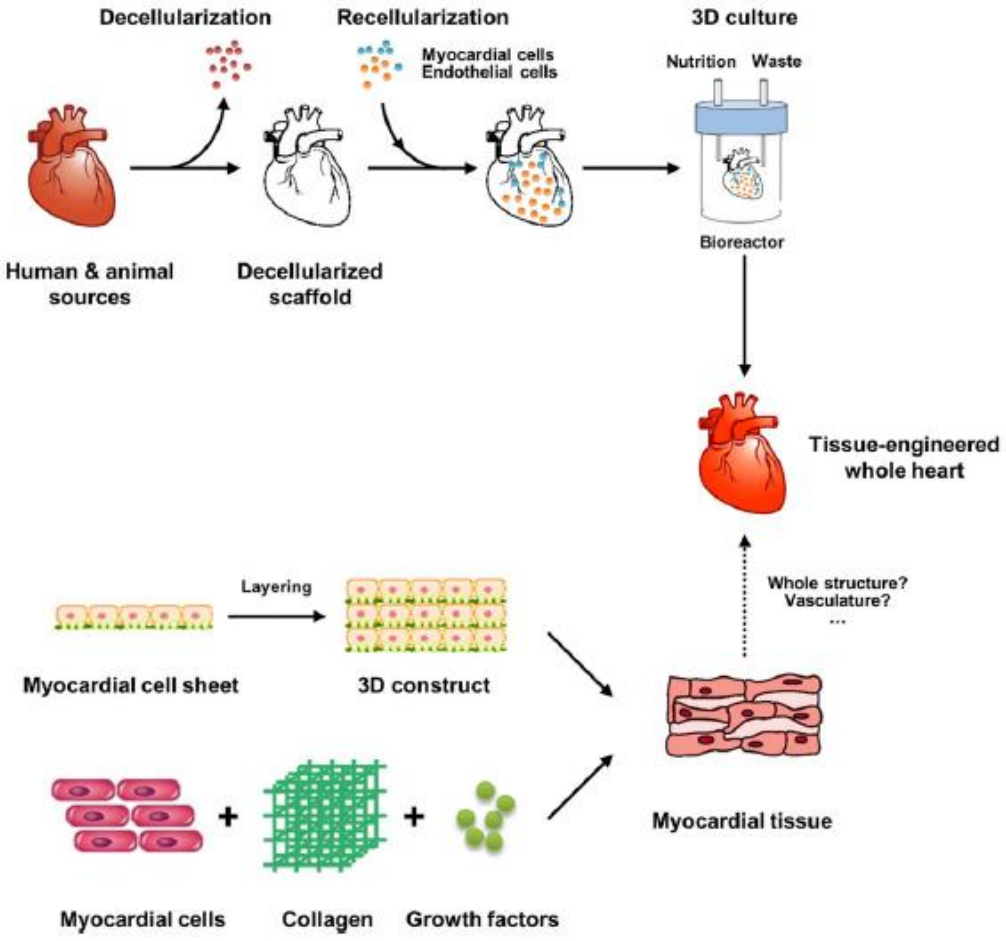

Figure 3 Construction strategies in heart tissue engineering. For the decellularization-based construction strategy, human or animal donor-derived hearts undergo the process of decellularization to obtain decellularized whole heart scaffolds with preserved macroarchitecture. Regenerative cells (e.g., myocardial cells and endothelial cells) are seeded onto decellularized scaffold through perfusion. Repopulated scaffolds are placed under 3D culture condition in a bioreactor, yielding tissue-engineered whole heart with overall structure and vasculature of heart. For the cell sheet-based construction strategy, 3D construct was produced by layering 2D myocardial cell sheets, leading to formation of myocardial tissue. For the synthetic/natural materials-based construction strategy, cells (e.g., myocardial cells), scaffolds (e.g., collagen), and growth factors are combined in vitro to produce myocardial tissue.
Adapted from (Zheng et al. 2018) with permission from John Wiley & Sons, Ltd.

1.5.1 Scaffold-based tissue engineering approaches

Many groups who took the scaffold-based approaches have sought to create tissue engineering scaffolds using polymer materials. A variety of materials have been studied including synthetic materials (e.g. polylactic acid (PLA) and polyglycolic acid (PGA) and their copolymers (Ozawa et al. 2002a and 2002b, Shin'oka et al. 2005), polyhydroxybutyrate (PHB) (Stock et al. 2000 and Malm et al. 1994), polyester urethane (PEUU) (Fujimoto et al. 2007)), as well as materials derived from biological sources (e.g. gelatin (Li et al. 1999 and Sakai et al. 2001), alginate (Gaetani et al. 2012)). These materials could be prepared in porous structures (e.g. sponges, meshes) (Zimmermann and Cesnjevar 2009) and could be formed as patches, conduits, and valves in order to be used for surgeries. Scaffolds are advantageous as it can support cell attachment and provide structural integrity during early stage of tissue regeneration, which is important when considering *in situ* cardiac tissue regeneration, as the implanted graft could be exposed to mechanical force under physiological conditions (Benrashid et al. 2016). The requirements for an ideal scaffold include the following attributes; biocompatible, has adequate mechanical strength while being pliable, can be sutured, has low incidence of immunological response, infections, calcification, and thrombosis, and has the capability to remodel into a functional tissue (Benrashid et al. 2016). Especially in the case of tissue engineering for CHD treatment applications, where patient growth is one of the important factors to consider, biodegradable/bioabsorbable materials are preferred as it is thought that the scaffold would eventually be replaced with a new tissue formed by the patient's own cells, which can grow with the patient. (Ozawa et al. 2002b). Hoerstrup et al. has demonstrated the potential of growth in a tissue-engineered vascular graft (TEVG) made by seeding myofibroblasts and endothelial cells to a PGA/PHB scaffold. They implanted the TEVG into a growing lamb model and

observed significant increase in diameter and length. Furthermore, histology indicated native-artery-like tissue formation. Degradation of PGA and PHB were confirmed during the 100-week follow up (Hoerstrup et al. 2006).

The efficacy of TEVG has been evaluated in clinical trials as well. A group from Tokyo Women's Medical University performed implantation of tissue engineered grafts to 42 patients since 2001. The engineered tissue graft was made by combining a copolymer of lactide acid and ε -caprolactone with a woven fabric sheet of poly-L-lactide acid (PLLA) or PGA. Autologous bone marrow cells (BMC) were seeded onto the graft prior to implantation. Short-term follow-up (median 16.7 months) reported satisfactory results where no graft-related complications occurred and the tube graft remained patent. The same group also conducted a long-term follow-up (mean 5.8 years) for 25 patients and reported that graft stenosis and thrombosis occurred in 4 and 1 patients, respectively. No aneurysm, graft rupture, infection or ectopic calcification were found (Shinoka et al. 2005 and Hibino et al. 2010). It is noteworthy that 96% of patients who received TEVG implantation were able to discontinue anticoagulation therapy after 6 months from the operation, while implantation of synthetic grafts (Dacron and Gore-tex) usually require long-term anticoagulation drugs (Hibino et al. 2010). As graft stenosis is one of the known complications that could occur in synthetic grafts as well, in other words, not specific to TEVG, it could be said that the reported results demonstrated the feasibility of tissue-engineered grafts and the potential benefits it may bring to CHD patients (Hibino et al. 2010).

To date, majority of scaffold-based tissue engineering studies employs cell-seeded graft approaches. Ozawa et al., who compared biodegradable (gelatin, PGA, Poly(ε- caprolactone-co-L-lactide): PCLA) and non-biodegradabe (PTFE) materials by implanting unseeded patches to a rat model in a manner that mimics right

ventricular outflow tract (RVOT) repair, reported that although host cell infiltration was observed in biodegradable patches after 8 weeks of implantation, they were predominantly fibroblast and collagen. As localized dilatation of vessels (e.g. aneurysms) occur in a similar fashion, considering risks, they suggested that cell-seeding on tissue engineering scaffolds prior to implantation may be essential (Ozawa et al. 2002).

Subsequently, several studies have reported interesting findings regarding the role of seeded cells. Roh et al. used a mouse model to elucidate the mechanism of tissue regeneration which was observed in human BMC-seeded TEVG. They found that the human cells seeded on the graft were not detectable from 1 week after the implantation. By comparing seeded and unseeded scaffolds, they demonstrated that the seeded human BMCs contributed to higher host cell recruitment via a paracrine mechanism. In particular, significantly high levels of monocyte chemotactic protein-1 (MCP-1) secretion were found in human BMC-seeded scaffolds. When MCP-1 microparticles were embedded in unseeded scaffold, significant improvement in host cell recruitment was observed (Roh et al. 2010). Furthermore, Hibino and colleagues demonstrated that the neotissue formed on the graft mainly consist of host-derived cells. Using a sex-mismatched chimeric mouse model, where the graft was seeded with male BMC and implanted to female CB57BL/6 mice, and the source of the cells which populated the TEVG was determined by detecting the Y chromosome (Hibino et al. 2011). The above findings indicate that cell-seeding to the graft is not indispensable. The authors claim that considering the burden which autologous cell harvest would cause to the patient and clinical staffs, a cell-free approach could be more beneficial (Hibino et al. 2011). Patterson et al. also suggested the advantage of cell-free tissue engineering grafts, referring to integration of TEVGs with controlled release systems of cytokines as a potential approach (Patterson et al. 2012).

Recently, Matsumura and colleagues have developed a cell-free TEVG and demonstrated its potential as *in situ* tissue engineering scaffold. The TEVG is composed of polyglycolide knitted fibers and a PCLA sponge reinforced with glycolide and ε-caprolactone copolymer (P(GA/CL)) monofilament. The TEVGs were implanted in a canine inferior vena cava (IVC) model and followed up for 24 months. Interestingly, the content of hydroxyproline, elastin, and calcium of the TEVG were comparable to that of native IVC. Moreover, histology indicated formation of vessel-like tissue. The authors attributed this success to the optimal mechanical properties and degradation time of the scaffold. In particular, in their previous studies, they observed that internal surface endothelialization of the scaffold occurs within a month after implantation, and that if fibrotic tissues massively proliferated during this initial period, it would lead to stenotic changes of the TEVG. Thus, they fabricated the scaffold as it would maintain its shape during the endothelialization period, which was achieved by the P(GA/CL) monofilament reinforcement. While the P(GA/CL) monofilament degraded within 2 months, the PCLA spongy scaffold degraded concurrently but more slowly, to maintain a relatively constant elasticity in the TEVG to support the tissue remodeling process. (Mastumura et al. 2012).

As discussed earlier, ECM has many advantages as a material for tissue engineering applications. SIS-ECM derived from porcine has been recently approved by the Food and Drug Administration (FDA) and has been introduced to cardiac surgery (Diagnostic and Interventional Cardiology n.d.). SIS-ECM is thought to serve as a bioscaffold which allows native cells of the implanted region to grow into the scaffold and regenerate native tissue (Kimura 2018). Clinical performance of SIS-ECM in CHD surgeries appears to be mixed results. Quarti et al. reported that none of the 26 patients who received SIS-ECM implantation experienced graft-related complications (Quarti et al. 2011). Similarly, Scholl et al. reported overall good

outcomes in the 40 patients they performed SIS-ECM implantation. Re-operation was required in one patient due to regurgitation of the tricuspid valve which was repaired using SIS-ECM. The explanted tissue exhibited signs of resorption of the SIS-ECM, replacement with organized collagen, and re-endothelialization which indicates the potential of SIS-ECM to be replaced by autologous tissue (Scholl et al. 2010). On the other hand, multiple groups have reported unsatisfactory results. Rosario-Quinones et al. reported that out of 25 cases where SIS-ECM were used in CHD surgery, 6 patients required reoperation, all exhibiting hemodynamically significant lesions at the site of the SIS-ECM implantation. Signs of intense inflammatory reaction with accompanying granulation tissue and fibrosis were observed in histological analysis of explanted specimens (Rosario-Quinones et al. 2015). Nelson and colleagues who used SIS-ECM patches as a hemi-Fontan baffle during the palliative procedure and subsequently explanted them as part of standard Fontan operation observed inflammatory responses in all explanted patches. Furthermore, they reported that none of the explanted specimens showed evidence of ingrowth of native cells to the SIS-ECM or transformation into cardiac tissue (Nelson et al. 2016). Similarly, Hofmann and colleagues reported 5 cases of valve insufficiencies out of 6 patients who received aortic valve procedures using SIS-ECM. No signs of the expected remodeling of SIS-ECM into native-like tissue were found in the explanted specimens (Hofmann et al. 2017). Zaidi et al. who examined the explanted SIS-ECM used for valve reconstruction in CHD also reported similar results. The authors suggested the discrepancy in outcomes could potentially be due to difference in location and manner of implantation, such as whether the SIS-ECM was in contact with native tissue or blood stream, normal or abnormal tissue (Zaidi et al. 2014). Clinical experiences are now accumulating, which may in the future aid identification of appropriate patients and indications to use SIS-ECM, and lead to improved outcome.

Along with clinical efforts, research to improve the efficacy of SIS-ECM is in progress. Tanaka and colleagues developed a SIS-ECM patch combined with a controlled release of basic fibroblast growth factor (bFGF) and compared its performance with pristine SIS-ECM and Dacron patches using a porcine model. Histological analysis suggested that bFGF-incorporated SIS-ECM enhanced ingrowth of host cells and constructive myocardial remodeling. Moreover, cardiac magnetic resonance measurement results as well as regional staining observations indicated early restoration of contractility and tissue perfusion in the bFGF-incorporated SIS-ECM compared to control patches (Tanaka et al. 2015).

While cardiac ECM have demonstrated promising potential in cardiac tissue repair for ischemic heart disease treatment, limited number of studies have reported its application for CHD treatment. Wainwright et al. used a cardiac ECM patch obtained by performing perfusion decellularization on porcine hearts to repair the full-thickness RVOT defect created in a rat model. After 16 weeks, the cardiac ECM patch remodeled from an acellular collagen-rich scaffold into a vascularized collagenous tissue with scattered small islands of cardiomyocytes. In contrast, Dacron patches implanted in the same manner were encapsulated by a thin dense connective tissue layer where little cellular infiltration was observed. As for cardiac function, cardiac ECM-patched hearts exhibited no difference in the size or function of the ventricles compared to baseline values, while dilation was observed in Dacron-patched hearts. The authors claim that it may be possible to achieve a contracting tissue by seeding stem cell-derived cardiomyocytes to this cardiac ECM patch (Wainwright et al. 2012), based on the success of a previous study where cardiomyocytes were seeded on SIS-ECM (Hata et al. 2010). This cardiac ECM patch utilizing whole-heart decellularization has two major advantages; (1) it allows preservation of macroscopic and ultrastructural properties which would be desirable

in terms of mechanical strength of the patch, and (2) it could be used to repair large defects which is impossible in the case of using autologous tissue (Wainwright et al. 2012). The limitation of this cardiac ECM patch approach could be the potential risk of immunological responses seen in xenograft implantation and the necessity to have a whole organ to be decellularized.

The approach of utilizing ECM hydrogels is advantageous in terms of creating an autologous ECM tissue engineering scaffold, as ECM hydrogels could be obtained from pieces of a tissue. However, for CHD treatment applications, where grafts in the form of sheets and conduits are required, its poor mechanical strength become a major challenge. A strategy to solidify the ECM hydrogel strong enough to form grafts is necessary. Although ECM solution is known to spontaneously gel via self-assembly of ECM components (Brightman et al. 2000), the resulting gel is usually too soft to form a graft. A common approach to increase mechanical strength of a hydrogel is to add crosslinking agents. Examples of commonly used crosslinking agents include genipin (Sundararaghavan et al. 2008), transglutaminase (Greenberg, Birckbichler, and Rice 1991), and glutaraldehyde (Jayakrishnan and Jameela 1999). In a study carried out by Wassenaar and colleagues demonstrated that the addition of genipin, glutalaldehyde, and transglutaminase, at the concentration of 1 mM, 0.05%, 120 mU/mL respectively, can increase the Young modulus of hydrogels without inducing cell toxicity (Wassenaar et al. 2016a). However, it is suggested that the crosslinking of these agents is still not sufficient to solidify the ECM hydrogels to form grafts (Williams et al. 2015). Strong crosslinking agents such as glutaraldehyde are known to have risks of cytotoxicity at higher concentrations (Jorge-Herrero et al. 1999). Based on unsatisfactory experience with moderate crosslinking agents, Williams and colleagues developed an ECM-fibrin hydrogel using transglutaminase as a crosslinking agent. In their study, because the ECM interfered with the crosslinking

of fibrins, the concentration of ECM was low as 0.34 mg/mL while fibrin was used at 3.3 mg/mL. Despite of the low ECM concentration, effect was observed on the differentiation of patient-derived cardiovascular progenitor cells when seeded on the ECM-fibrin hydrogel (Williams et al. 2015), which indicates the potential of this ECM hydrogel approach. Interestingly, difference in gene expression of cardiovascular differentiation markers (VWF and CNN1) was found when ECM-fibrin hydrogels prepared from ECM derived from neonatal and adult rats were compared (Williams et al. 2015). A potential cause for this would be the remodeling of ECM which is suggested to take place during aging. In a previous study carried out by Wiiliams et al., where a shotgun proteomics was performed on cardiac ECMs derived from fetal, neonatal, and adult rats, significant difference in ECM composition between neonatal and adult rats were found (Williams et al. 2014).

In summary, based on previous studies, cardiac ECM has potential advantages as a material for CTE. However, when considering utilization of ECM hydrogels obtained via decellularization of tissue pieces, for CHD treatment applications, a strategy to crosslink the hydrogel to form a graft material with sufficient mechanical strength is necessary.

1.5.2 Scaffold-free tissue engineering approaches

Scaffold-free approach is based on the self-assembly of cells. An example would be the cell sheet technique, where cells are first cultured on a surface coated with a temperature sensitive polymer (poly(N-isopropylacrylamide), PIPAAm). Once cells become connected to each other, the cultured cell sheet could be lift off by solubilizing the PIPAAm coating by simply lowering the temperature. Cell sheets could be stacked to fabricate a three-dimensional contractile tissue (Shimizu et al. 2006) (**Figure 3**). Although the reported study was not specifically aiming for CHD treatment applications, it may have the potential to be utilized in the future.

Scaffold-free approach could be beneficial in terms of cell density, as the resulting sheet would be a compact myocardium similar to native tissue (Tee et al. 2010), as well as in terms of elimination of risk of immunological reaction to the foreign scaffold material.

1.5.3 Decellularization-recellularization approach

Decellularization-recellularization approach was reported by Ott et al. in 2008. Using cadaveric rat hearts, decellularization of whole heart was carried out by performing retrograde coronary perfusion of detergent solutions. The decellularized heart preserved the perfusable vascular architectures and structures of valves and chambers as well as the ECM components. The decellularized heart was subsequently seeded with cardiac or endothelial cells and successfully attained generation of pump function of the heart (Ott et al. 2008) (**Figure 3**). This approach has the potential to allow generation of artificial hearts using xenogeneic hearts, which may supply the shortage in donors for heart transplantation (Tee et al. 2010).

1.5.4 Biotubes

Another unique and promising approach is the biotube method. This is based on the tissue encapsulation phenomenon of foreign materials which occur in living bodies. Kato et al. reported a case of clinical application to a 2-year-old CHD patient. 19 F drain tubes were embedded in the subcutaneous space, as a mold for biotube formation during a palliative surgery performed prior to defect repair. After 8 months, the biotube was retrieved, and by cutting longitudinally, a tissue patch could be obtained. The patch was used for right pulmonary artery augmentation. Computed tomography (CT) images showed that after 9 months of implantation, the shape of the augmented pulmonary artery was well preserved, and no aneurysm formation nor stenotic change were observed (Kato et al. 2016).

1.6 Proteomics on ECM

To date, the intricate and dynamic cell-ECM interaction is not yet fully understood. Many studies have showed evidence of ECM-remodeling taking place under the influence of diseases. Therefore, a deeper understanding of the ECM proteome may provide valuable insights into pathophysiology, which may lead to improvement in treatment by allowing identification of novel prognostic and diagnostic markers and therapeutic opportunities (Naba et al. 2015). Additionally, having a better understanding of the ECM may aid development of bioinspired CTE approaches. Proteomics is a powerful technique to globally characterize the proteome and have been employed widely to understand the pathophysiology of various diseases. While many studies have been carried out to understand the ECM proteome and to study the influence of diseases in the field of cancer and cardiovascular diseases (Lindsey et al. 2016), only limited number of proteomic studies have been reported on CHD (Xia et al. 2013, Bond et al. 2018a and 2018b). Xia and colleagues have performed a shotgun proteomics on cardiac tissue obtained from CHD patients to understand the right ventricular (RV) remodeling seen among pediatric CHD patients by comparing tissues obtained from TOF and non-TOF patients. By gene ontology analysis, they found an increase in levels of glycolysis-related proteins and a decrease in lipid-metabolism-related proteins in tissues obtained from TOF patients. Moreover, they found one of the ECM proteins, lumican, to be more abundant in non-TOF tissue compared to TOF tissue in the results of proteomics and subsequently confirmed by western blot (Xia et al. 2013). Lumican is known to be involved in regulation of collagen fiber assembly and fibrosis seen in ischemic and reperfused hearts (Fasso et al. 2008). Xia et al. also identified several other ECM proteins (biglycan, collagen alpha-1(XIV) chain, collagen alpha-6(VI) chain, EGF-containing fibulin-like extracellular matrix protein 1, emilin-2, fibulin-5,

fibrinogen beta chain, and fibrinogen gamma chain) as differentially expressed in TOF tissue in their shotgun proteomics results (Xia et al. 2013). It should be noted that the protein profile reported by Xia had some discrepancies compared to the results reported in previous studies using animal models. As a potential cause for this discrepancy, the authors pointed out the difference between human CHD and the traditional pulmonary artery banding animal model, in its pathophysiological process, time to progression, and molecular basis. They also referred to the potential influence caused by age, treatment, and other complications in the case of human subjects (Xia et al. 2013). Their findings depict the limitation in the usage of animal models to understand the dynamic nature of ECM and indicate the value of studying specimens obtained from human subjects.

Bond and colleagues analyzed the RV tissues obtained from patients with VSD and TOF to compare the effect of different causes of RV disfunction. While VSD patients have RV hypertension due to the presence of left-to-right shunt, TOF patients have obstruction in RV. Gene ontology with enrichment analysis revealed that TOF patients had higher expression of proteins which are involved in contractile mechanisms. Some ECM proteins were identified in their studies, where none of them found to be differentially expressed (Bond et al. 2018a). The ECM protein identified in their study comprised approximately 1-2% of the total identified proteins, which seems to be lower than one could expect, given that collagen constitutes 30% of total protein mass of a multicellular animal (Frantz, Stewart, and Weaver 2010).

Generally, when shotgun proteomics are performed on whole tissue, the predominance of intracellular constituents hamper identification and accurate quantification of ECM proteins (Lindsey et al. 2016). Therefore, to study ECM proteins by shotgun proteomics, depletion of abundant proteins (i.e. removal of

intracellular proteins) is usually required. Furthermore, proteomics on ECM is challenging due to the insoluble and tightly packed nature of ECM proteins which hinder sufficient protein extraction and digestion. To the author's knowledge, no studies have performed proteomics on cardiac ECM of pediatric CHD patients.

1.7 Objective of this study

This study consists of three parts; (1) decellularization of cardiac tissue obtained from pediatric CHD patients, (2) creation of ECM hydrogel as a CTE scaffold for CHD treatment and (3) establishment of a sample preparation procedure to perform proteomic analysis on cardiac ECM of pediatric CHD patients. To the author's knowledge, this would be the first attempt to carry out these tasks.

In this study, cardiac ECM hydrogel sheets were created by combining ECM derived from pediatric CHD patient tissues and gelatin methacrylate (GelMA). The incorporation of patient-derived ECM is thought to help mimicking the cell-ECM interaction in the hydrogel, as it would contain various macromolecules which are present in the natural ECM. GelMA was selected as a crosslinking agent, as it has demonstrated its capability to fabricate a hydrogel sheet for CTE in previous studies carried out by Nikkhah laboratory (Navaei et al. 2016 and 2017 and Saini et al. 2015). By utilizing photopolymerization of GelMA, hydrogels can be formed into a sheet that could be peeled off from the glass on which it was prepared. In a previous study, where GelMA was combined with gold nanorods (GNRs) to make a CTE scaffold, it was demonstrated that GNR-GelMA hydrogel exhibited good cell adhesion property and allowed cardiac tissue formation with organized sarcomeric α- actinin structures and expression of connexin 43 gap junction protein. It was suggested that the incorporation of GNRs improved cell adhesion by increasing the stiffness of the hydrogel as well as by providing anchoring points for cells to adhere (Navaei et al. 2016).

Based on the results of the previous studies on hydrogels of ECM and GelMA-GNR, it was hypothesized that the ECM-GelMA hydrogel would exhibit improved cell retention compared to pristine GelMA hydrogel and would facilitate cardiac tissue formation. To investigate this hypothesis, ECM-GelMA hydrogels were created and the functionality was evaluated. Evaluation include cell retention, viability, expression of cardiac specific markers, and beating behavior of the cultured cells. In addition, based on the finding from the previous study where addition of GNRs to GelMA hydrogels enhanced cell maturation (Navaei et al. 2016 and 2017), the effect of incorporating GNR into ECM-GelMA hydrogel was investigated.

As for the establishment of sample preparation procedure for proteomic analysis, a previously reported approach which performs serial digestion using cyanogen bromide (CNBr) and trypsin was employed, and the quality of peptide generation was assessed by SDS-PAGE and matrix assisted laser desorption/ionization (MALDI).

CHAPTER 2

DECELLULARIZATION OF CARDIAC TISSUE OBTAINED FROM PEDIATRIC CHD PATIENTS

2.1 Introduction

A large number of studies on decellularization of cardiac tissue has been reported, most of which is for animal tissues. Generally, decellularization could be carried out by treating the tissue with decellularization reagents. Chemical reagents, such as acids and bases, hypotonic and hypertonic solutions, chelating reagents and detergents (e.g. SDS) are used to lyse cell membranes and to remove cytosolic and genomic material (Hussey et al. 2018 and Crapo, Gilbert, and Badylak 2011). Alcohols (e.g. methanol and isopropyl alcohol) could be used for delipidization. In addition, proteases (e.g. trypsin, collagenase) and nucleases (e.g. ribonuclease (RNase) and deoxyribonuclease (DNase)) are used to digest cell debris and residual nucleic acids (Hussey et al. 2018 and Crapo, Gilbert, and Badylak 2011). Treatment with decellularization reagents could be carried out by either agitated immersion of the minced tissue, or in cases where a whole heart could be obtained, perfusion using the vessels could be an option (Ott et al. 2008). Four articles which carried out decellularization of human cardiac tissue were identified (Johnson et al. 2014 and 2016, Godier-Furnémont et al. 2011, and Oberwallner et al. 2014). Johnson et al. carried out decellularization by treating the tissue with phosphate buffered saline (PBS) solution containing 1% SDS for several days followed by DNase/RNase treatment. Godier-Furnemont and colleagues on the other hand, first performed lysis using a solution containing 10mM of tris(hydroxymethyl)aminomethane-hydrochloride (Tris-HCl) and 0.1% of ethylenediaminetetraacetic acid (EDTA) and then treated with 0.5% SDS solution followed by DNase/RNase treatment. Oberwallner et al. proposed a slightly modified version of Godier-Furnemont's

group's method, where fetal bovine serum (FBS) was used as a substitute for nuclease. All four reports used adult cardiac tissue and no reports on decellularization of cardiac tissue of pediatric patients were found. In this study, the protocol reported by Johnson et al. (Johnson et al. 2014, Johnson et al. 2016) was employed.

Successful decellularization is usually evaluated based on the removal of cellular components, by measures including hematoxylin and eosin staining, immunostaining using 4',6-diamidino-2-phenylindole (DAPI), and quantification of residual double-stranded DNA (dsDNA). Multiple studies employ the threshold reported by Crapo et al, where <50 ng dsDNA/mg per dry weight ECM is defined as the threshold based on the potential to cause immunogenicity (Crapo, Gilbert, and Badylak 2011). The chemical reagents used in decellularization would affect ECM proteins as well, therefore, some portions of ECM components would be removed during decellularization. Therefore, optimal decellularization is a matter of balance between sufficient removal of cellular components to minimize risk of immunogenicity, and the retention of ECM components. Quantification of ECM components such as glycosaminoglycans, collagen and elastin are often carried out to assess the retention of ECM components (Oberwallner et al. 2014, Dijkman et al. 2012, Schulte, Simionescu, and Simionescu 2013, Methe et al. 2014, and Wainwright et al. 2010). However, in this study, quantification of ECM components was not feasible due to the limited amount of ECM that could be obtained from each patient. Alternatively, ECM retention was qualitatively confirmed by Movat pentachrome staining and immunostaining. Movat pentachrome staining allows visualization of collagen, elastin, fibrin, and the nuclei. Immunostaining was performed for two components; collagen type I and laminin. Collagen type I is known to be the most abundant protein in the cardiac ECM (Villarreal and Kim 1998) and to serve as a

backbone of the ECM. Laminin is a basement membrane protein which is known to take part in regulation of cell adhesion, migration, differentiation and proliferation (Hamill et al. 2009).

2.2 Materials and methods

2.2.1 Decellularization of human cardiac tissue

This study was approved by the Institutional Review Board (IRB) of Phoenix Children's Hospital (PCH). Cardiac tissue was obtained from pediatric CHD patients who underwent a planned surgery or biopsy at PCH as part of standard treatment. Tissue of ventricular, including left and right, from total eight patients were obtained. Decellularization was carried out following an established protocol. (Johnson et al. 2014 and 2016). Briefly, the tissues specimens were minced into 3-5 mm size pieces and treated with 1% SDS in Dulbecco's phosphate buffered saline (DPBS) solution for 6-8 days on a shaker at room temperature until the color of the tissues turns to pure white. After shaking in distilled water (DW) for 24 hours, the tissues were treated with a DNase/RNase solution for 24 hours at 37 °C to remove the residual cellular components. The DNase/RNase solution contained 40U/mL of DNase, 1U/mL of RNase, 40 mM of Tris-HCl, 6mM of magnesium chloride, 1 mM of calcium chloride, and 10 mM of sodium chloride and the pH was confirmed to be between 7 to 8. The tissue was then washed with 1% SDS/DPBS for 24 hours to

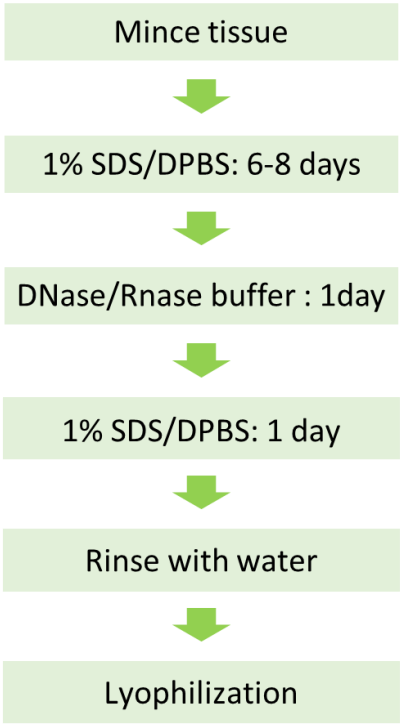

Figure 4
Decellularization process of cardiac tissue

remove the residual DNase and RNase, followed by 24 hours of rinsing in DW. Finally, the tissue was thoroughly rinsed with DW, lyophilized, and stored at -80 °C until usage (**Figure 4**).

2.2.2 Quantification of residual DNA

DNA was extracted using NucleoSpin Tissue XS kit (Macherey-Nagel) following the manufacturer's advice. 1mg of ECM was used and 8 μL of protenase K was added twice (upon initiation of lysis and after 3 hours) for complete lysis of the sample. The extracted DNA was quantified using Quanti-iT Picogreen dsDNA assay (Invitrogen).

2.2.3 Immunostaining for collagen type I and laminin

For native tissue, cryopreservation was carried out using 30% sucrose prior to freezing. Cryosections of 5 μm thickness were prepared from both, native and decellularized tissue. Fixation was performed before staining, by submerging the samples with 4% paraformaldehyde solution in DPBS for 15 minutes followed by three washes in DPBS. Primary monoclonal antibodies for collagen type I and laminin were obtained from Santa Cruz and Abcam, respectively. Secondary antibodies; goat anti-mouse Alexa Fluor-488 for collagen type I and goat anti-rabbit Alexa Fluor-555 or 594 for laminin was purchased from Life Technologies. Permeabilization was performed using 0.1% Triton X-100 for 15 minutes, followed by five washes with DPBS. The samples were then blocked using 10% goat serum (Life Technologies). Next, primary antibodies for collagen type I and laminin, prepared at dilutions of 1:100 and 1:200 respectively, were applied and samples were incubated overnight at 4 °C, followed by five washes with DPBS. Secondary antibodies were both prepared at dilution of 1:200 and applied for 1 hour. After five washes with DPBS, DAPI (Life Technologies, 1:1000 dilution in DPBS) staining was performed and fluorescent images were taken using Zeiss Axio Observer Z1 at 10x objective.

2.2.4 Histological evaluation

Preparation of 5 μm cryosections and fixation was performed in the same manner as described in section 2.2.3. Movat pentachrome staining was performed using a kit (Cancer Diagnostics) following the manufacturer's advice. Images were obtained using Nikon Elipse TE300 Inverted Video Microscope (Nikon).

2.3 Results and discussion

Total of eight tissue specimens obtained from PCH were decellularized. DNA quantification was performed in all samples, except for one which the amount of obtained decellularized tissue was too small. In all seven decellularized samples, the amount of residual dsDNA was found to be below 50 ng per 1 mg of dry ECM, indicating sufficient removal of cellular components. Results of immunostaining were in accordance, as no nuclei could be identified in DAPI staining nor Movat pentachrome staining in decellularized tissue (**Figure 5 and 6**).

Retention of ECM components were assessed by immunostaining and Movat pentachrome staining. Immunostaining was performed for collagen type I and laminin, as these proteins are known to be one of the main components of the interstitial ECM and basal lamina, respectively. Both are known to have motifs to which a vast range of macromolecules could bind to (Lodish et al. 2000), therefore, both are important components to facilitate cell-ECM interaction. As seen in **Figure 5**, although the fine structures observed in native tissue is lost after decellularization, both collagen type I and laminin appeared to be present in decellularized tissue. These observations are in accordance with previous studies where decellularization was performed using SDS (Ott et al. 2008, Godier-Furnémont et al. 2011, Oberwallner et al. 2014, and Singelyn et al. 2009). In Movat pentachrome staining (**Figure 6**), removal of muscle cells (round components stained red) and retention of collagen (stained yellow) were also observed. Fibrins

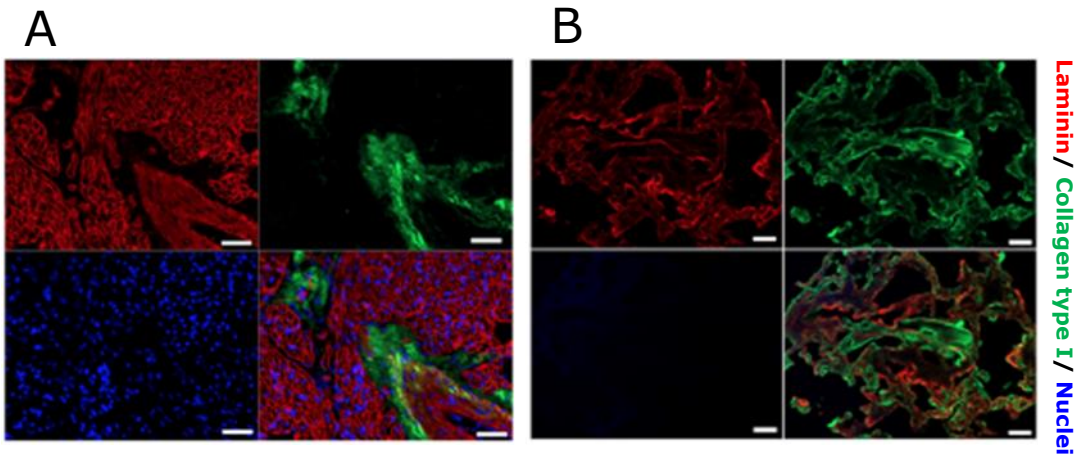

Figure 5 Representative fluorescent images of native (A) and decellularized tissue (B). Laminin, collagen type I, and nuclei are stained red, green, and blue, respectively. Scale bars represent 50 μm.

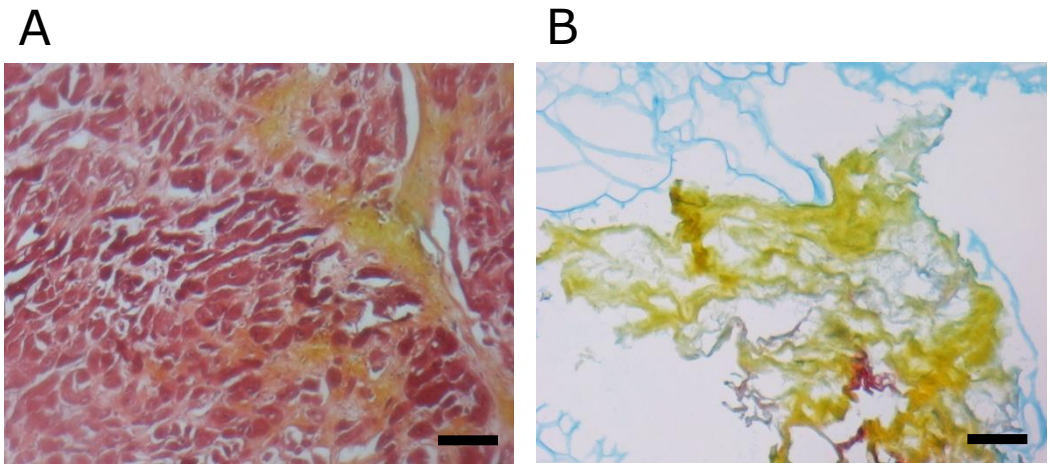

Figure 6 Representative images of Movat pentachrome staining of native (A) and decellularized tissue (B). Collagen are stained yellow and muscle and fibrin are stained red. The blue mesh-like structure is agarose which was used upon sectioning. Scale bars represent 100 μm.

(small fibrils stained red) which were identified in native tissue could not be found in decellularized tissue. It is not clear whether this indicate the loss of fibrin during decellularization procedure, or it is due to the sample preparation procedure for staining. As seen in **Figure 6A,** fibrins are small fibrils which is not homogeneously distributed, thus, identification could depend on the location where cryosections were

obtained. In addition, while native tissue is sectioned in a manner which the original structure is preserved as much as possible, decellularized tissue have undergone extensive washes and lyophilization prior to sectioning and staining. Considering these factors, it was difficult to assess the fibrin retention based on staining.

In summary, sufficient removal of cellular components was confirmed in the decellularized tissues. Collagen and laminin appeared to be present after decelluarization, however, the retention of ECM components could not be assessed sufficiently in the staining experiments carried out. It could be expected that if proteomic analysis could be performed in the future, that could be an alternative method to confirm retention of ECM proteins.

CHAPTER 3

FABRICATION OF ECM-INCORPORATED GELATIN-BASED HYDROGEL

3.1 Introduction

As discussed earlier, utilization of ECM hydrogel for CHD treatment applications requires a strategy to crosslink the ECM hydrogel to form a graft. Moderate crosslinking agents which are often used, such as genipin (Sundararaghavan et al. 2008) and transglutaminase (Greenberg, Birckbichler, and Rice 1991), are suggested to be not sufficient to increase the mechanical stiffness of the hydrogel (Williams et al. 2015). Strong crosslinking agents (e.g. glutaraldehyde (Jayakrishnan and Jameela 1999)) are known to have higher risk of cell toxicity at high concentrations.

GelMA was selected as a crosslinking agent for this study, as it has multiple advantageous aspects as a material for tissue engineering applications. First, it is biocompatible. As gelatin is denatured collagen, it retains many of the bioactive features of collagen, including cell binding motifs and MMP-sensitive degradation cites (Nichol et al. 2010), which are both important in facilitating cell-ECM interaction. In multiple previous studies carried out by Nikkhah laboratory, GelMA hydrogel successfully accommodated cardiac cells allowing them to form a cardiac tissue with contractile properties (Navaei et al. 2016 and 2017 and Saini et al. 2015). Furthermore, long-term (49 days) cell viability has been confirmed in an experiment using porcine aortic valvular interstitial cells (Benton et al. 2009). Second, the methacrylate group allow photopolymerization and the physical properties (mechanical stiffness and swelling property) of the resulting hydrogel can readily be tuned by the adjusting the degree of methacrylation during synthesis, or the GelMA concentration in the hydrogel (Nichol et al. 2010). In this study, GelMA with high degree of methacrylation (96.41 ± 1.54%) (data not shown) was used at the concentration of 5%. This concentration was chosen considering the results of a

previous study which found a decrease in cell viability when higher concentrations (10 and 15%) were used (Nichol et al. 2010), as well as the results of a preliminary experiment where 2.5% was found insufficient to form a sheet structure.

3.2 Materials and method

3.2.1 Preparation of solubilized ECM

Cardiac tissues (left ventricle and left ventricular septum) obtained from one pediatric CHD patient was used for this experiment. The tissue was snap frozen upon arrival from PCH. Frozen tissue was thawed and cut into 3-5 mm pieces, and decellularization was carried out in the same manner as described in section 2.2.1. To 10 mg of lyophilized ECM, pepsin solution (1 mg/mL in DW) was added and the ECM was homogenized using Precellys 24 and Hard Tissue Homogenizing CK28 (Bertin Instruments). The ECM homogenate was transferred to a scintillation vial with a stirrer and 8.3 uL of 1M hydrochloric acid (HCl) was added. Final volume was adjusted to 1 mL and digestion was carried out for 48-72 hours at room temperature under stirring, until the ECM particles disappeared. Upon completion of digestion, the solubilized ECM was neutralized with 1M NaOH and aliquoted into centrifuge tubes. Finally, the aliquots of solubilized ECM were frozen at -80 °C followed by lyophilization and stored at -80 °C until usage.

3.2.2 Synthesis of Gelatin methacrylate

GelMA was synthesized following previously established protocol (Nichol et al. 2010 and Navae et al. 2016 and 2017). Briefly, type A gelatin (Sigma-Aldrich) (10% w/v) was dissolved in DPBS at 50 °C. This was followed by dropwise addition of 8% v/v methacrylic anhydride (Sigma) and the solution was stirred for 3 h at 50 °C. The methacrylation reaction was terminated by diluting the solution with DPBS at 50 °C. The final solution was purified by dialysis using a 12-14 kDa molecular weight cutoff dialysis tube. Dialysis was performed at 45 °C in DW under stirring for 7 days.

Finally, the dialyzed solution was filtered using a 0.2 μm membrane, followed by lyophilization.

3.2.3 Synthesis of gold nanorods

GNRs were synthesized following an established protocol of seed mediated growth method (Nikoobakht and El-Sayed 2003 and Navaei et al. 2016 and 2017). Briefly, 2 mL of hydrogen tetrachloroaurate ($HAuCl_4$) aqueous (0.5 mM in DIW) solution was first mixed with 2 mL of 0.2 M hexadecyltrimethylammonium bromide (CTAB) solution (0.2 M in DW), resulting in a deep yellow solution. 240 μL of ice-cold sodium borohydride ($NaBH_4$) dissolved in DW was added at once to the solution under stirring and the mixture was kept stirred for 2 minutes. Immediately after adding $NaBH_4$, the color of the solution turned from deep yellow to light brown-yellow, which indicated the formation of gold nanoparticles (seed solution). The seed solution was incubated for at least 4 hours at 30 °C. Next, the growth solution was prepared in a falcon tube by adding 1.12 mL of silver nitrate ($AgNO_3$) (4 mM in DW) to 20 mL CTAB (0.2 M in DW) followed by the addition of $HAuCl_4$ (1 mM in DW) solution 20 mL, resulting in a deep yellow solution. 280 μL of ascorbic acid solution (13.88 mg in 1 mL DW) was added and the solution was mixed by inverting the falcon tube, turning the solution colorless. Finally, 48 μL of seed solution was added into the growth solution at 30 °C and kept incubated overnight. The color of solution turns to brown-red over a period of half an hour, indicating the formation of GNRs. Based on transmission electron microscopy images, the average aspect ratio of the synthesized GNRs was calculated to be approximately 3.15 (data not shown). To remove excess CTAB, the synthesized GNRs colloid was centrifuged at 12,000 rpm for 10 min and washed with DPBS twice.

3.2.4 Preparation of ECM-GelMA-GNR hybrid hydrogels

First, photoinitiatior ((2-hydroxy-1-(4-(hydroxyethoxy) phenyl)-2-methyl-1-propanone; Sigma) was dissolved in DPBS at the concentration of 0.5% w/v. This solution was added to lyophilized GelMA (final concentration 5% w/v) and the mixture was kept at 80 °C until complete dissolution was confirmed. The GelMA solution was then kept at 40 °C until usage. For ECM-GelMA hydrogels, the GelMA solution was added to lyophilized ECM to result in final concentration of 2.4% of ECM. 1.2%ECM-GelMA solution was prepared by diluting the 2.4%ECM-GelMA solution with GelMA solution. For the GNR-incorporated hydrogels, necessary amount of GNRs to result in a final concentration of 1 mg/mL in the hydrogel was aliquoted and centrifuged at 12,000 rpm for 10 minutes. The supernatant was removed and hydrogel solutions (GelMA or ECM-GelMA) were added. The mixture was mixed thoroughly by votexing to disperse the GNRs.

Hydrogel constructs were prepared via photopolymerization. First, 6 μL of the ECM-GelMA-GNR mixture was pipetted on a plastic surface, between two 150 μm tall spacers, and covered with a glass slide coated with 3-(trimethoxysilyl) propyl methacrylate (TMSPMA; Sigma). The construct was formed by exposing this setup to UV light (800 mW, 360–480 nm). When the TMSPMA coated glass are removed, the hydrogel construct would detach from the plastic surface and the spacers, resulting in the hydrogel to be retrieved attached on the TMSPMA coated glass.

Prior to cell culture experiments, the constructs were treated with 2% v/v penicillin-streptomycin (100 units/mL) in DPBS for 10 min twice followed by 10 min incubation in DPBS and another 10 min incubation in cardiac cell culture medium. Cell culture medium used in this study contained Dulbecco's modified eagle medium (DMEM) (Gibco), FBS (10%) (Gibco), L-Glutamine (1%) (Gibco), and penicillin-streptomycin (100 units/mL) (1%).

3.2.5 Cardiomyocytes isolation and culture

Cardiomyocytes were obtained from two days old neonatal rats following an established protocol approved by Institution of Animal Care (IACUC) at Arizona State University (ASU) and based on previous extensive expertise of Nikkhah laboratory (Navaei et al. 2016 and 2017 and Saini et al. 2015). Briefly, the thorax of the neonatal rats was opened, and hearts were harvested. Upon removing the atria, the hearts were cut into 3–4 medium sized pieces and placed in 0.05% trypsin solution (without EDTA; Gibco) prepared in Hank's balanced salt solution (HBSS; Gibco) for approximately 16 hours at 4 °C with continuous gentle shaking. Next, the heart pieces were neutralized in cell culture medium and further treated with type II collagenase, yielding a mixture of cardiomyocytes and cardiac fibroblasts. The cell suspension was then preplated in T-175 flasks to isolate cardiomyocytes. After an hour of preplating, most of the cardiac fibroblasts attach to the flask, while cardiomyocytes remain unattached. Unattached cells were collected and used for experiments.

Hydrogel constructs were placed in a 48-well plate and harvested cardiomyocytes were seeded on top (6.0×10^5 cells/well). Cells were cultured in the cardiac culture medium for 8 days. Culture medium was changed every other day.

3.2.6 Evaluation of cell of retention and survival

Cell retention was evaluated by the fraction area of the hydrogel covered by cells at day 1 of culture. 10x magnification images were obtained from at least 3 individual locations per construct. More than quadruplicate samples were evaluated for each condition per experiment, and experiments were repeated 4 times.

Cell viability after 8 days of culture was evaluated using standard Live/Dead assay kit (Life technologies, USA) following the manufacturer's instruction. A solution containing 0.5 µL of calcein AM and 2 µL of ethidium homodimer in 1 mL of warm

DPBS was applied to the cells for 30 min. Fluorescent z-stack images at 10× magnification were taken to visualize live cells (stained green) and dead cells (stained red). Cell viability was calculated by dividing the number of live cells by the total number of cells.

All images were acquired using a phase-contrast/fluorescence microscope (Zeiss Axio Observer Z1) equipped with Apotome, and subsequent analysis (calculation of fraction area covered by cells and counting of live/dead cells) were performed using NIH ImageJ software.

3.2.7 Analysis of beating behavior of the cells

The spontaneous beating of cardiomyocytes was monitored from day 1 to day 8 of culture. Using a phase-contrast microscope (Zeiss Axio Observer Z1), a 30 seconds-long video was recorded for each sample at 2.5x magnification. Representative beating signals were acquired from images of five individual locations using a custom written MATLAB code used in a previous study (Navaei et al. 2016).

3.2.8 Immunostaining for cardiomyocyte specific markers (sarcomeric α-actinin and connexin 43)

Primary monoclonal antibodies for sarcomeric α-actinin and connexin-43 were obtained from Sigma and Abcam, respectively. The secondary antibodies; goat anti-mouse Alexa Fluor-488 for sarcomeric α-actinin and goat anti-rabbit Alexa Fluor-555 for connexin 43 were both purchased from Life Technologies. At day 8, cardiomyocytes were fixed with 4% paraformaldehyde for 30 min, followed by five washes in DPBS. Permeabilization was carried out by applying 0.5% Triton X-100 for 45 min at room temperature. Next, cells were blocked in 10% goat serum for 2 hours at room temperature. Primary antibodies for both sarcomeric α-actinin and connexin 43 were prepared in 10% goat serum at 1:100 dilution. After applying the primary antibodies, samples were kept at 4 °C overnight followed by five washes in

DPBS. As for secondary antibodies, Alexa Fluor-488 anti-mouse and Alexa Fluor-555 anti-rabbit were both prepared at 1:200 dilution in 10% goat serum (Life Technologies) and applied for 1 hour. Cells were then washed three times with DPBS. Finally, cells were stained with DAPI (Life Technologies, 1:1000 dilution in DPBS) for 10 minutes to label the nucleus followed by three washes in DPBS. Fluorescent z-stack images were obtained using a fluorescence microscope (Zeiss Axio Observer Z1) equipped with Apotome at 40x- objective.

3.2.9 Statistical analysis

All the data collected in this study were analyzed using one-way ANOVA analyses and reported as mean ± standard deviation (SD). Turkey's multiple comparison with a p-value < 0.05 was employed to evaluate statistically significant difference between groups. All statistical analyses were performed using GraphPad Prism (v.6, GraphPad).

3.3 Results and discussion

3.3.1 Fabrication of ECM-GelMA hydrogel

The incorporation of neither ECM (1.2% or 2.4%) nor the GNRs (1 mg/mL) interfered with the crosslinking of GelMA, and constructs of six conditions were fabricated successfully. The conditions will be referred as stated in parenthesis hereinafter; Pristine 5% GelMA hydrogel (5%GelMA), 5% GelMA hydrogel containing 1 mg/mL of GNRs (GelMA-GNR), 5% GelMA hydrogel containing 1.2% of ECM (1.2%ECM-GelMA), 1.2%ECM-GelMA containing 1 mg/mL of GNRs (1.2%ECM-GelMA-GNR), 5% GelMA hydrogel containing 2.4% of ECM (2.4%ECM-GelMA), 2.4%ECM-GelMA containing 1 mg/mL of GNRs (2.4%ECM-GelMA-GNR). The hydrogel constructs were prepared to have the height of 150 μm, and the diameter was approximately 5 mm among all conditions.

3.3.2 Cell retention and viability

Cell retention was evaluated at day 1 of culture, based on the fraction area of hydrogel covered by cells. **Figure 7** shows the results of four repeated experiments. A large between-experiment variability was observed, and no statistically significant difference was found among the six conditions. However, in 3 out of 4 experiments, ECM-incorporated hydrogels showed significantly higher cell retention compared to pristine GelMA, which may indicate that the addition of ECM may have a slight effect on cell retention of the hydrogel. More experiments may be necessary to assess whether that trend could be constantly observed.

The viability at day 8 also exhibited a large variability between experiments and no statistically significant difference was found (**Figure 8**). Although an almost significant difference was found when comparing ECM2.4%-GelMA and ECM2.4%-GelMA-GNR ($p=0.0634$), given the large variability seen in the cell retention in four experiments as shown in **Figure 7**, as well as the observations noted during experiments where viability tend to be low when cell retention was low, it was deemed to be inappropriate to assess the effect at this point with small number of experiments ($n=3$).

The large between-experiment variability can be attributed to several factors. First would be the quality of cardiomyocytes which could vary by the quality of cell isolation. Second would be the between-batch variation in the composition of solubilized ECM. Although the solubilized ECM used in the experiments were all prepared from the tissue obtained from a single patient, decellularization and solubilization were carried out in several batches. In addition, the specimen contained the left ventricle as well as the left ventricular septum, and ECM composition could differ depending on which part of the tissue was used. Protein removal which takes place during decellularization as well as the digestion efficiency

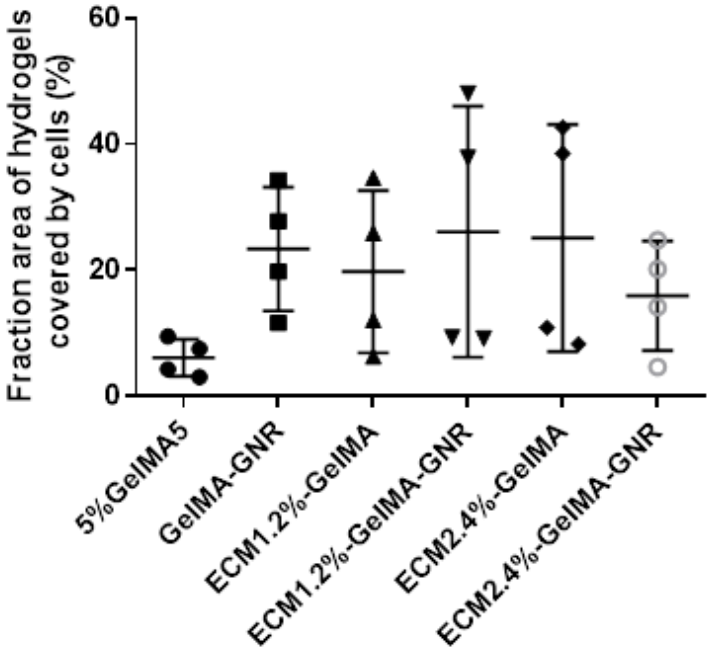

Figure 7 Cell retention. Cell retention is calculated by the fraction area of hydrogels covered by cardiomyocytes at day 1.

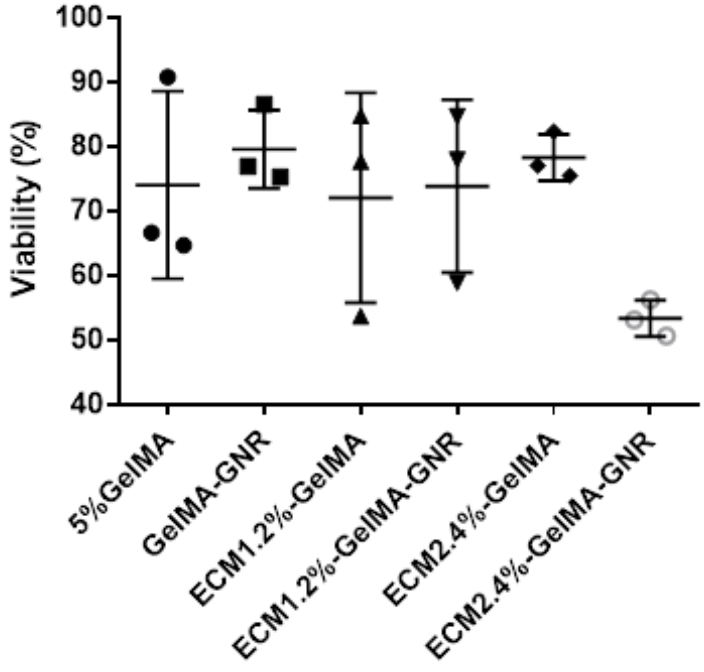

Figure 8 Viability of cardiomyocytes seeded on ECM-GelMA-GNR hydrogels at day 8 of cell culture.

using pepsin could be impacted by the variability in the ECM composition of the sample. Batch-to-batch variability is a well-known limitation in ECM-based materials (Romano et al. 2011, Serban and Prestwich 2008). Third is the heterogenous nature of ECM hydrogels. As mentioned earlier, spontaneous gelation of ECM hydrogels could occur at 37 °C via self-assembly of ECM components. During preparation of ECM-GelMA-GNR hydrogels, GelMA was warmed to 40 °C prior to mixing with ECM. Therefore, spontaneous gelation could occur during mixing the hydrogel solution prior to photo-crosslinking. During the experiment, it was observed that some of the hydrogel constructs contained few small pieces of ECM.

In summary, cell retention and viability were found to have a large between-experiment variability and the results were inconclusive at this point. However, it would be worth noting that the cells appeared to spread more in hydrogels containing ECM and/or GNRs compared to pristine GelMA hydrogel (**Figure 9**), which observation was consistent among the four experiments carried out.

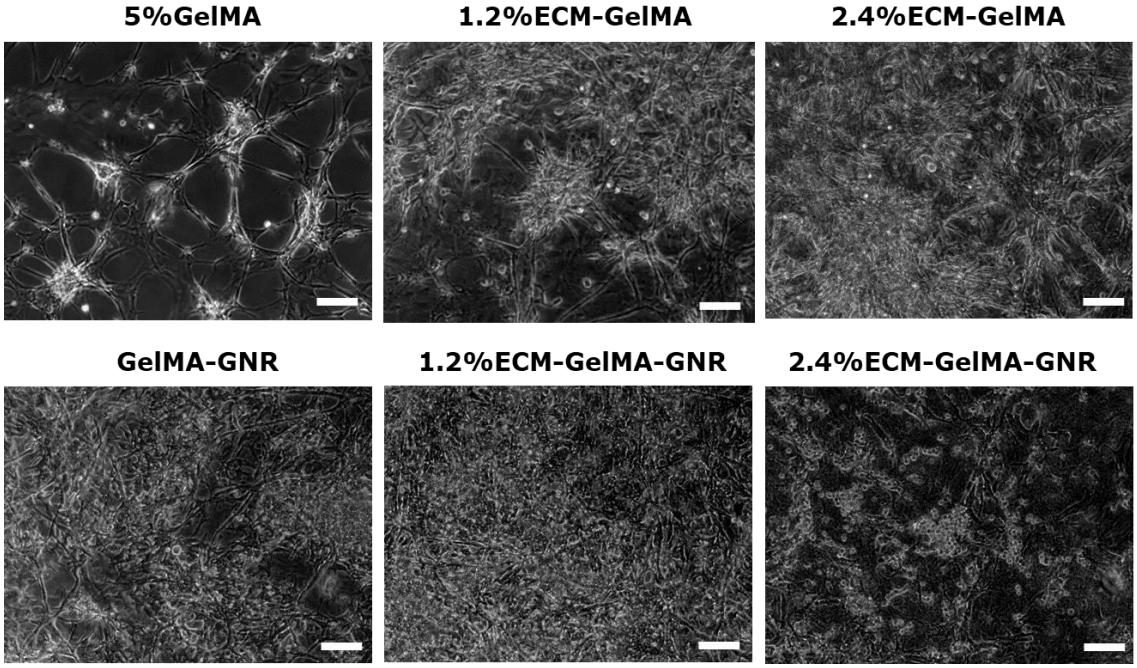

Figure 9 Representative phase-contrast images of the hydrogels at day 8 of cell culture. Scale bars represent 100 μm.

3.3.3 Assessment of spontaneous beating behavior

Beating is a phenomenon observed during culture of cardiomyocytes. At initial time points of cell culture, cardiomyocytes individually beat spontaneously. As cells spread and connect to each other, gap junctions will be formed and cell-cell coupling will be established. By cell-cell coupling, cardiomyocytes become able to beat in a synchronous manner (i.e. cardiomyocytes at different locations of the hydrogel beat synchronously), which gives the appearance of the hydrogel as a "spontaneously beating sheet". Thus, the occurrence of synchronous beating could indicate the presence of cell-cell coupling. Establishment of cell-cell coupling would be a sign of cell maturation as it allows the connected cells (i.e. formed tissue) to beat synchronously in response to external electrical stimuli, just as the native heart tissue. However, it should be noted that spontaneous beating involves stochastic factors, such as the presence of pacemaker cells. Therefore, the lack of spontaneous beating does not necessarily mean insufficient cell-cell coupling. **Figure 10** shows representative beating signals of spontaneous beating observed at day 8. Beating signals were obtained from five individual locations from each construct. Although variability was observed in beating behavior, such as frequency of beating and the fraction of hydrogel beating, majority of the hydrogels exhibited synchronous beating at day 8. Interestingly, when ECM and GNRs were incorporated, the frequency of spontaneous beating tend to be lower compared to the cases where either ECM or GNRs was incorporated. One potential cause could be the difference in cell adhesion and spreading. During experiments, it was observed that the ECM-GelMA hydrogels tend to have more cell clusters compared to ECM-GelMA-GNR hydrogels, which could potentially be indicating difference in cell-ECM interaction. Further study would be necessary to investigate what factors (e.g. anchoring points, stiffness of hydrogel) may have caused this difference.

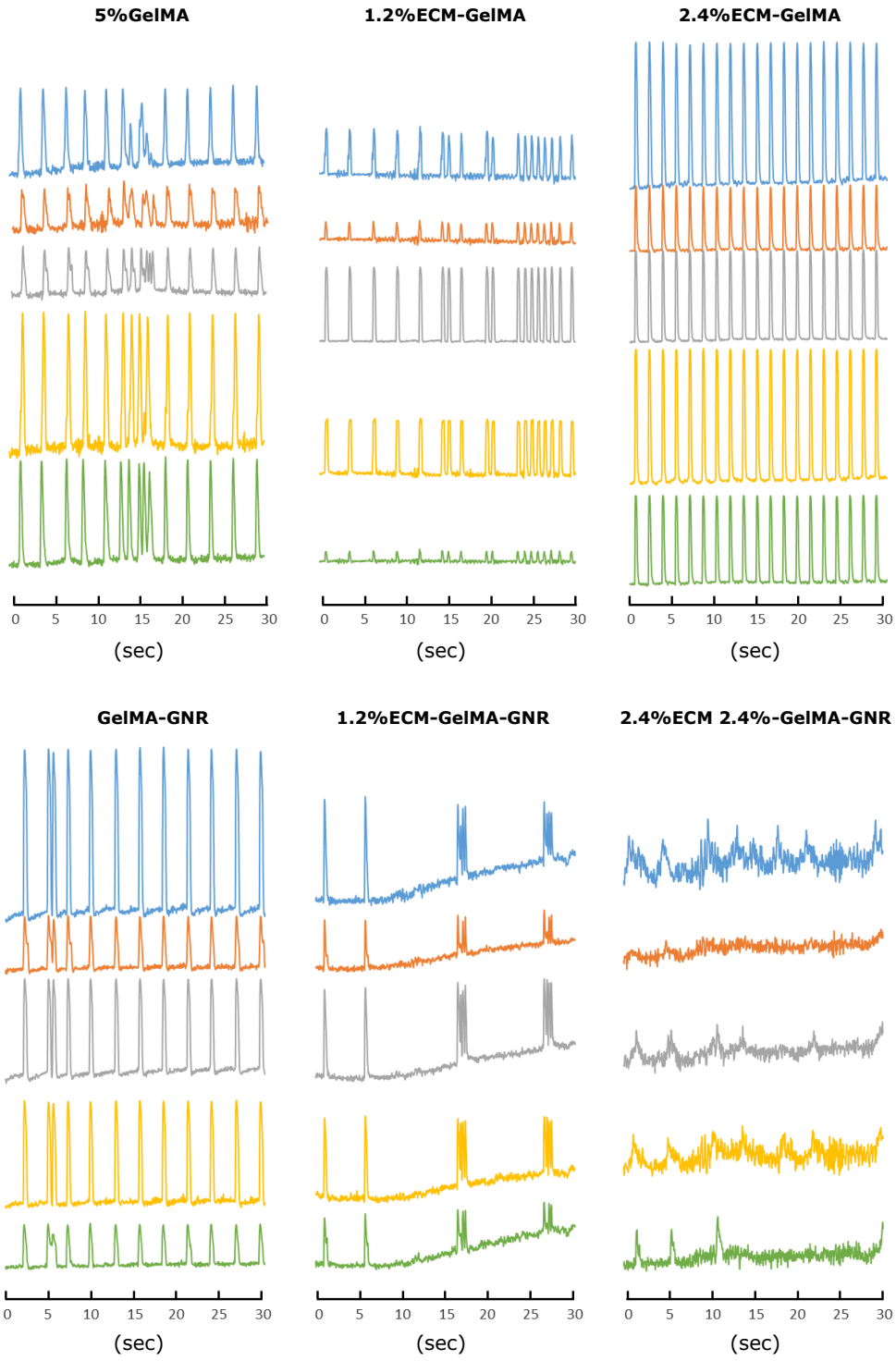

Figure 10 Representative spontaneous beating signals at day 8 of cell culture. Beating signals obtained from five individual location are shown.

.

3.3.4 Expression of sarcomeric α-actinin and connexin 43

Phenotype of cultured cardiomyocytes was assessed by immunostaining for cardiac specific markers, sarcomeric α-actinin and connexin 43. Sarcomeric α-actinin takes part in the actin-myosin contraction complex, and connexin 43 is a gap junction protein known to be responsible for synchronous contraction of the cells (Oyamada et al. 1994). As can be seen in **Figure 11**, organized sarcomeric α-actinin structures and expression of connexin 43 were evident in hydrogels containing ECM and/or GNRs. Although there was variability, presumably due to the variability in cell spreading, the trend where expressions of cardiac specific markers were evident in ECM- and/or GNRs-incorporated hydrogels compared to pristine GelMA hydrogel, was constantly observed.

The beneficial effect of adding GNRs to GelMA hydrogel was in accordance with the results of the previous studies (Navaei et al. 2016 and 2017). Multiple previous

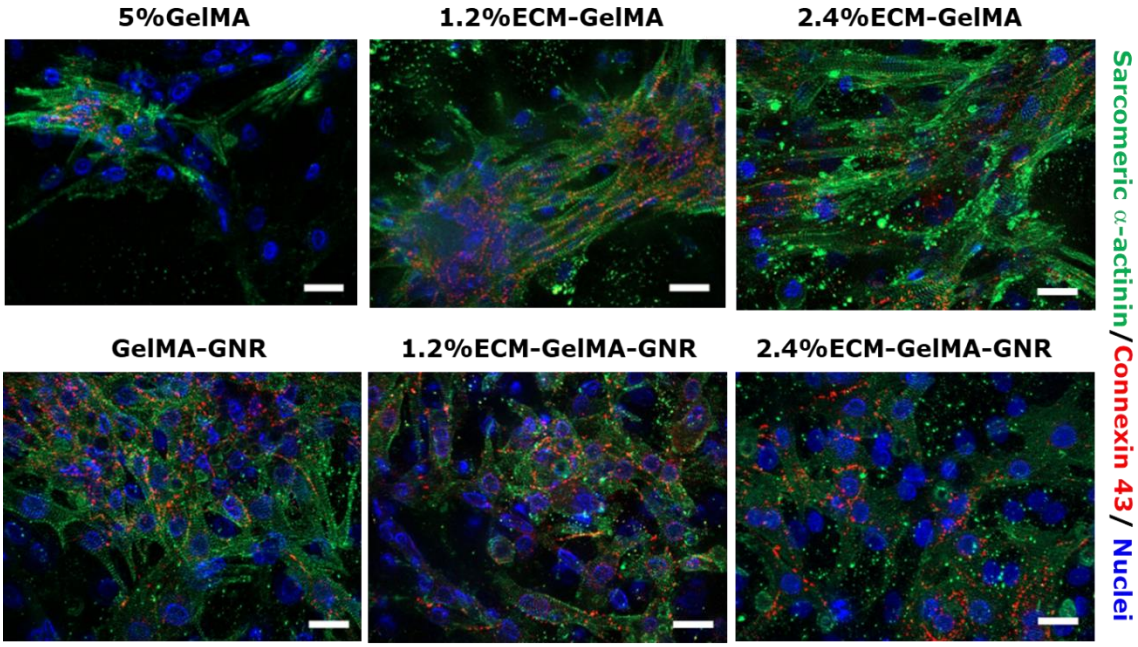

Figure 11 Representative fluorescent images of immunostaining for cardiac specific markers. Sarcomeric α-actinn are stained red and connexin 43 are stained green. Scale bars represent 25 μm.

studies have reported that the addition of nanomaterials to polymer hydrogels would enhance cell maturation, where alteration in nano-scale surface topology and mechanical strength of the scaffold polymer have been suggested to be potential causes. Particularly, in the case of incorporating conductive nanomaterials to non-conductive polymer hydrogels, improved conductivity is thought to be another factor which may affect cell maturation, as it may facilitate electrical stimuli propagation in the hydrogel (Dvir et al. 2011, You et al. 2011, Pok et al. 2014, Li et al. 2014, and Navaei et al. 2016 and 2017). ECM, as described earlier, contains various proteins that could serve as motifs for cells to adhere, as well as regulators of cellular processes. Therefore, the higher expression of sarcomeric α-actinin and connexin 43 observed in hydrogels containing ECM and/or GNRs seems to be expectable and reasonable.

It should be noted that the expression of sarcomeric α-actinin and connexin 43 appeared to be comparable among hydrogels containing both ECM and GNRs, and those containing either of ECM or GNRs, despite the difference seen in spontaneous beating behavior. As shown in **Figure 10**, the later exhibited synchronous and periodical spontaneous beating, which was not prominent in the former. This indicates that the lack of spontaneous synchronous beating is not due to insufficient cell maturation and cell-cell coupling. Further study would be necessary to investigate the cause of the different beating behaviors. There could be a possibility that the combination of three components (GelMA, ECM, and GNRs) may have affected cellular processes responsible for cell spreading as well as spontaneous beating, in a different manner from two-component hydrogels (GelMA-ECM and GelMA-GNR). In addition, interactions between ECM and GNRs could be another possibility.

CHAPTER 4

OPTIMIZATION OF SAMPLE PREPARATION FOR PROTEOMICS

4.1 Introduction

Proteomics on ECM is a challenging task due to the characteristic features of ECM proteins, such as high molecular weight of the proteins and the presence of covalent protein crosslinks by which the ECM proteins become insoluble and difficult to extract (Hansen et al. 2015). Protein extraction from tissue materials, where proteins are already assembled into stable structures, is even more challenging. Sufficient extraction and digestion of ECM proteins are crucial for successful ECM proteomics (Hansen et al. 2015). While protein extraction using chaotropes and detergents is the most common method in bottom-up proteomics, various approaches, such as serial extraction using solutions of salts, chaotropes, and detergents (Barallobre-Barreiro et al. 2012 and Suna et al. 2018), ultra-sonication-assisted digestion (Hansen et al. 2015), and CNBr cleavage (Kraft, Mills, and Dratz 2001, Johnson et al. 2014 and 2016, and Vit et al. 2016) have been reported to address the difficulties in protein extraction. Hill et al., who aimed to accurately characterize the ECM, pointed out that protein extraction using chaotropes and detergents constantly yield an insoluble protein-containing pellet, which would be discarded prior to trypsin digestion. By employing chemical digestion with CNBr, they found nearly 80% of the fibrillar proteins (e.g. collagen type I, fibrillin-1) within the insoluble pellet remaining unextracted by chaotropes (**Figure 12**, Hill et al. 2015). The use of CNBr has several advantages. First, CNBr specifically cleaves proteins at the C-terminal of methionine (Vit et al. 2016), which specificity is important in proteomics. Second, ECM proteins include tightly packed hydrophobic proteins which could hinder enzymatic digestion facilitated by proteases (Hill et al. 2015 and Hansen

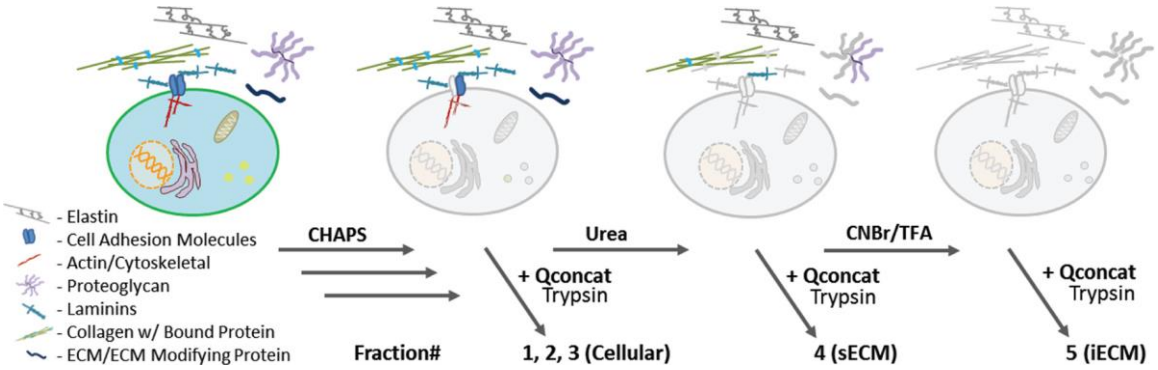

Figure 12 Effectiveness of protein extraction method. Cellular proteins are extracted using a high salt CHAPS buffer and mechanical tissue homogenization, solubleECM (sECM) is extracted using a 6 M urea buffer with vortexing and insolubleECM (iECM) is extracted after chemical digestion. Adopted by (Hill et al. 2015) with permission from ELSEVIER.

et al. 2015). This would not be a problem in the case of chemical digestion (Hill et al. 2015). Thirdly, as methionine cleavage sites are typically located in hydrophobic domains, cleavage at these points reduces the size of the hydrophobic fragments (Kraft, Mills, and Dratz 2001), and thus, could potentially improve protein extraction.

Building on the findings of the study carried out by Hill et al., Johnson and colleagues carried out proteomics on cardiac ECM of human adults by first decellularizing the tissue followed by serial digestion using CNBr and trypsin, and successfully characterized the cardiac ECM (Johnson et al. 2016).

In this study, the protocol reported by Johnson et al. was adopted to perform proteomics on cardiac ECM of pediatric CHD patients. Since it is suggested that ECM composition differ by age and the influence from diseases (Kraft, Mills, and Dratz 2001 and Williams 2014), it is unclear whether this protocol which was optimized for adult cardiac tissue would be applicable for pediatric CHD patient tissue as well. As a first step, whether the same protocol can generate peptides viable for proteomic analysis was assessed by SDS-PAGE and MALDI.

4.2 Materials and methods

4.2.1 Sample preparation for MALDI

Tissue obtained from one patient was used in this experiment. Tissue was snap frozen upon arrival from PCH and decellularized in the same manner as described in section 2.2.1, lyophilized and kept at -80 °C until usage.

Upon chemical digestion, 2-4 mg of lyophilized ECM was homogenized in 250-700 μL of water. Mixture of CNBr and trifluoroacetic acid (TFA) was added to the homogenate to result in a final concentration of 100 mM CNBr and 86% TFA. Chemical digestion was carried out at room temperature in dark for 24 hours. Subsequently, the volume of the sample was reduced under vacuum, and solvent exchange with water was performed three times. The resulting peptides were dissolved in water and the peptide concentration was measured by BCA assay (Thermofisher Scientific).

Trypsin digestion was performed by in-solution digestion, after chemical digestion. First, 50 μg of peptide was aliquoted and the solvent was removed using Speed-Vac. Next, the peptides were re-dissolved in 100 μL of 8M Urea in 50 mM Triethylammonium bicarbonate (TEAB) and 200 mM tris(2-carboxyethyl)phosphine (TCEP) was added to the final concentration of 10 mM. Reduction was carried out at 55 °C for 1 hour. The samples were then alkylated with iodoacetamide (final concentration 17 mM) at room temperature for 30 minutes in dark. Prior to trypsin digestion, the samples were diluted 5-times by adding 100 mM TEAB. 1 μg of trypsin was added to 10 μg of protein and digestion was carried out overnight at 37 °C. Digestion was quenched by the addition of 10% TFA to adjust the sample to pH lower than 2. The digested peptides were desalted using a desalting column (Thermofisher Scientific) prior to MALDI analysis. MALDI was performed using AB

SCIEX 4800 MALDI TOF/TOF MS mass spectrometer (SCIEX) and carried out by the Mass Spectrometry Core Facility of Arizona State University.

4.2.2 SDS-PAGE

SDS-PAGE was performed with a 15% Tris-Glycine gel. 10-20 μg of protein was loaded per well.

4.3 Results and discussion

As shown in **Figure 13**, the extracted ECM proteins mainly consist of high molecular weight proteins (higher than 100 kDa) (lane A). The standard in-solution trypsin digestion (i.e. protein extraction with urea followed by reduction, alkylation and trypsin digestion) (lane B) was able to generate peptides. However, the size appears to range at 5-40 kDa, which indicates that the generated peptides were large. Generally, peptides smaller than 10 kDa (preferably below 5 kDa) are required to perform mass spectrometry. In addition, during treating the ECM by this method,

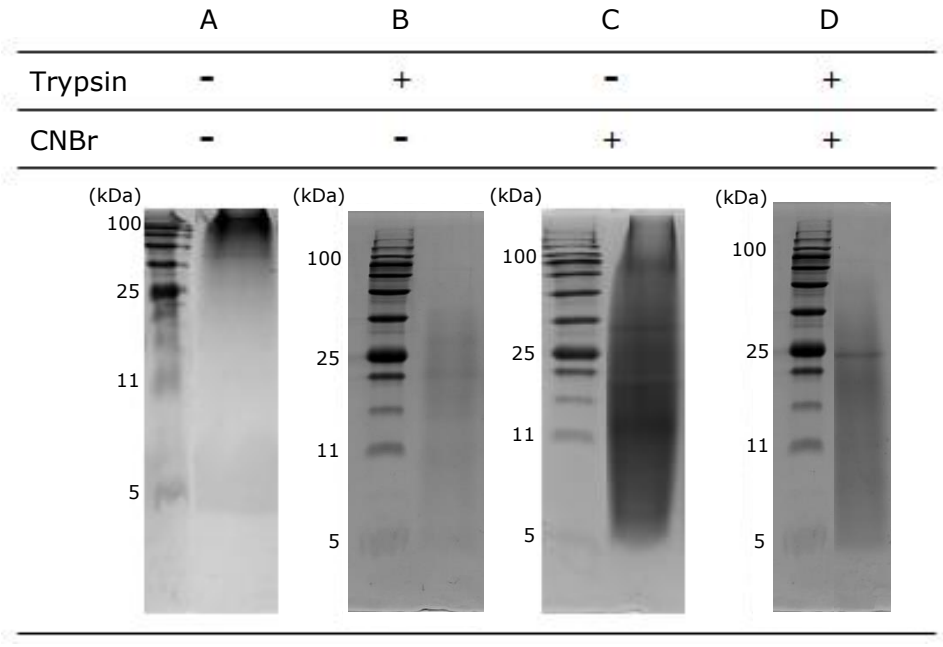

Figure 13 Comparison of digestion efficiency by SDS-PAGE. Undigested proteins extracted using 8M urea (A), digested with trypsin (B), treated with CNBr (C), and serially digested by CNBr and trypsin (D).

after protein extraction, an insoluble pellet was observed, which was in accordance with the observation reported by Hill et al. (Hill et al. 2015). This could be due to the tightly packed structure of ECM proteins as referred in previous studies (Hill et al. 2015 and Hansen et al. 2015). CNBr cleavage was able to break down the proteins to some extent and generated peptides with a wide range of size (lane C). Since the SDS-PAGE result revealed the presence of small peptides (<10 kDa) in the CNBr-cleaved samples, subsequent trypsin digestion was carried out by in-solution digestion instead of the filter-aided sample preparation (FASP) protocol which was employed in the protocol reported by Johnson et al. (Johnson et al. 2014 and 2016) to minimize peptide loss (i.e. the small peptides would be lost as flow-through during the centrifugation performed in FASP protocol to remove unwanted reagents). Serial digestion using CNBr and trypsin (lane D) generated smaller peptides compared to the case of performing CNBr-cleavage or trypsin digestion solely. Although sizes of peptides ranged up to 25 kDa, the majority appeared to be below 10 kDa, therefore, the sample was subjected to MALDI analysis to confirm the presence of peptides. The mass spectrum obtained by MALDI is shown in **Figure 14**. Although some peaks were detected, it was concluded that the digestion protocol requires further optimization, for the following reasons.

To validate this serial digestion method, bovine serum albumin (BSA) was treated in the same manner as the actual sample and evaluated by SDS-PAGE and MALDI (**Figure 15**). The SDS-PAGE exhibited a band below 10 kDa. Accordingly, more peaks were identified in MALDI, compared to the case of ECM. However, when a peptide mass fingerprint database search was attempted, BSA did not come up in the results. One potential cause could be low digestion efficiency. As the 3 large peaks seen at 1481, 1568, and 2046 (m/z) matches with the peaks in theoretical spectra, it could be interpreted that the cleavage by CNBr and trypsin is taking place,

however, the efficiency could be low resulting in low sequence coverage. Therefore, it was deemed that further optimization of this protocol is necessary.

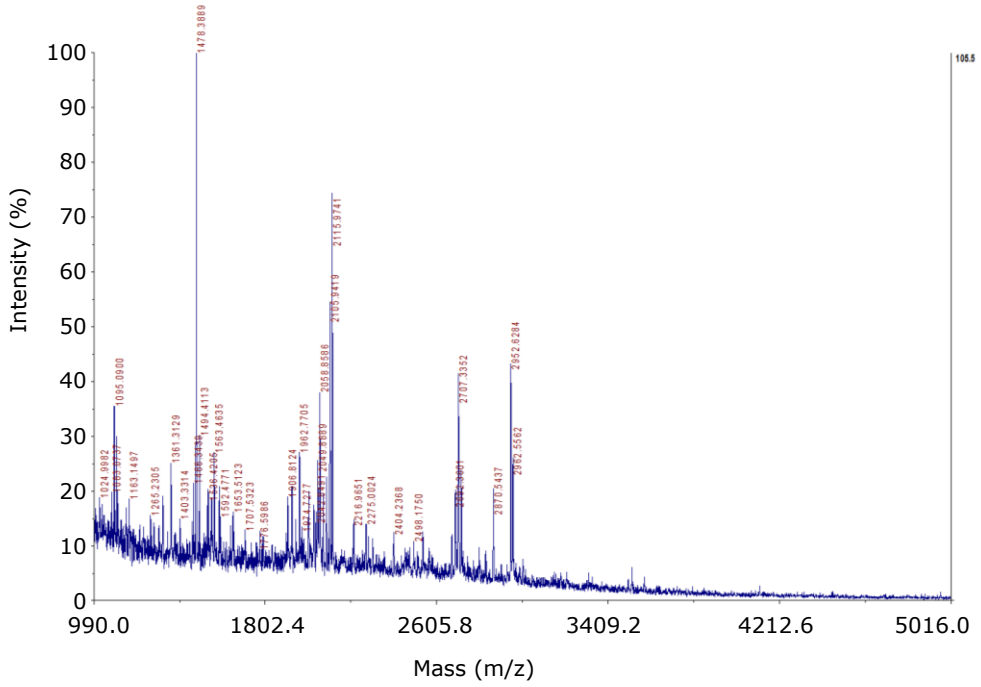

Figure 14 Mass spectrum of ECM

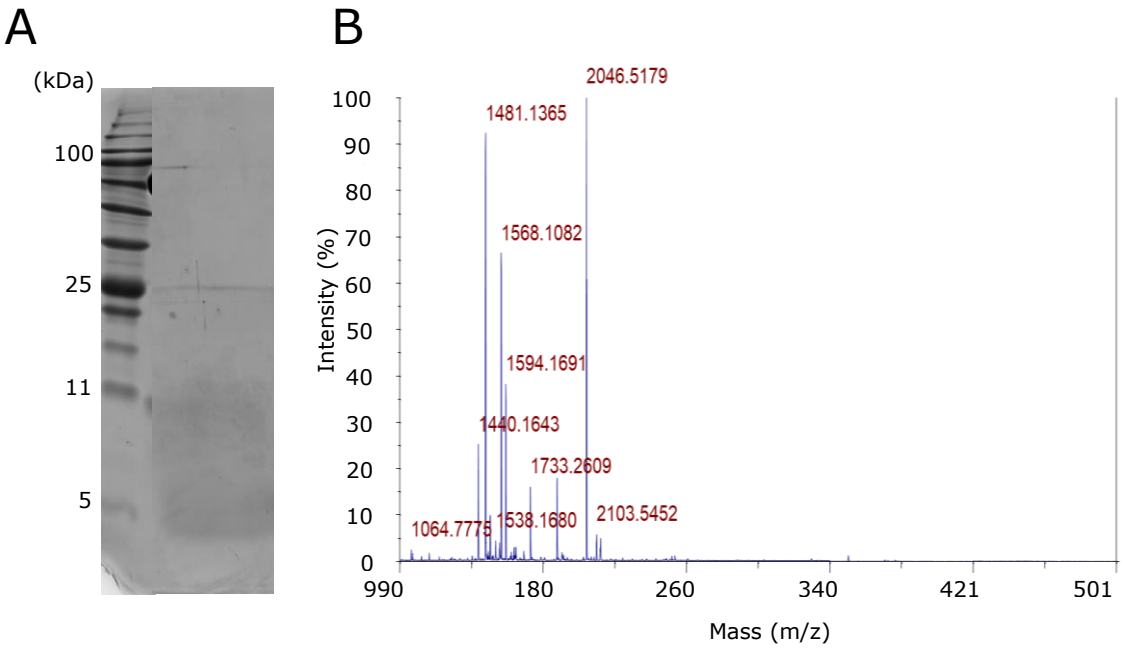

Figure 15 SDS-PAGE (A) and Mass spectrum (B) of BSA

CHAPTER 5

CONCLUSION AND FUTURE WORK

5.1 Conclusion

To the best of the author's knowledge, this is the first study to perform the followings; (1) decellularization of cardiac tissue obtained from pediatric CHD patients, (2) development of a patient-derived ECM and GNR-incorporated hydrogel for CTE applications, and (3) attempt made to prepare samples for proteomic analysis on cardiac ECM of pediatric CHD patients.

First, as for decellularization, it was confirmed that the cellular component was successfully removed by the procedures carried out in this study. Due to the limited amount of ECM sample that could be obtained by decellularization, quantitative evaluation on retention of ECM components was not feasible and qualitative assessment (histology and immunostaining) were able to identify only few ECM components (collagen and laminin). Nonetheless, the retention of those ECM components was confirmed, and the observations were in accordance with those reported in other analogous studies (Ott et al. 2008, Godier-Furnémont et al. 2011, Oberwallner et al. 2014, and Singelyn et al. 2009). If proteomics could be carried out in the future, it may serve as an alternative method to confirm retention of ECM proteins.

Next, ECM-GelMA-GNR hydrogel sheet was successfully created. Immunostaining for cardiac-specific markers revealed organized sarcomeric α-actinin structure and connexin 43 expression in the hydrogels containing ECM and GelMA, which indicated enhancement in cell maturation under the presence of these components. These results indicated the potential of ECM-GelMA-GNR hydrogels as a tissue engineering scaffold.

Interestingly, the spontaneous beating behavior of the cultured cells at day 8 was different depending on composition of the hydrogel. Given that signs of cell maturation and gap junction formation were confirmed by immunostaining in the hydrogels which did not beat, it could be speculated that the hydrogel composition may have influenced cellular processes responsible for cell spreading and spontaneous beating (i.e. contraction of cells). Further studies would be necessary to understand the mechanism of this interesting phenomenon.

As for evaluation on cell retention and variability, results were inconclusive as a large between-experiment variability was observed, which was potentially due to the variability inherent to experiments which employ cell isolation and ECM-based materials, as well as the variability caused by the experimental procedure.

5.2 Future Work

5.2.1 Experiments to evaluate applicability of ECM-GelMA-GNR patch to CHD treatments

As this is a preliminary proof of concept study which demonstrated the feasibility of tissue regeneration on this ECM-GelMA-GNR hydrogel, further studies would be necessary to judge the applicability of this approach to CHD treatments. First, physicochemical characterization, including mechanical strength and material degradation to assess the capability of the hydrogel patch to withstand surgery would be necessary. Second, due to time constrain, other concentrations of GelMA, ECM, and GNRs were not explored. Such experiments may be helpful not only in terms of determining the optimal composition, but also to understand the underlying mechanism of the observations. Third, *in vivo* study to evaluate the followings would be necessary; a) whether host cell would infiltrate into ECM-GelMA-GNR hydrogel, b) potential of the hydrogel to transform into a native-like tissue, and c) the growth potential of the newly formed tissue. These three points are particularly important to

address the unmet need in CHD surgeries; a graft that could integrate with the patient's heart and grow with the patient.

5.2.2 Experiments to understand the interactions between cells, ECM, GNR, and GelMA.

It was observed that when three components (ECM, GNR, and GelMA) were combined, the spontaneous beating behavior of the cultured cells differed from the case of the two-component hydrogel (ECM-GelMA, GelMA-GNR), which is an interesting phenomenon. A further investigation utilizing different approaches, such as evaluation on gene/protein expression, may give valuable insights to understand the underlying mechanism of the phenomenon as well as clues to further improve the effectiveness of this ECM-GelMA-GNR hydrogel approach.

5.2.3 Proteomics on cardiac ECM of CHD patients

This study was able to achieve the very first step of sample preparation for proteomics; generation of peptides from tissues of pediatric patients with CHD. As described above, further optimization to increase digestion efficiency would be necessary.

REFERENCES

Agmon, Gillie and Karen L. Christman. 2016. "Controlling stem cell behavior with decellularized extracellular matrix scaffolds." Current Opinion in Solid State and Materials Science 20: 193–201.

Alberts, Bruce, Alexander Johnson, Julian Lewis, Martin Raff, Keith Roberts, and Peter Walter. 2002. Molecular Biology of the Cell. 4th edition. New York: Garland Science.

American Heart Association." About congenital heart defects." n.d. Accessed on September 19, 2018. http://www.heart.org/en/health-topics/congenital-heart-defects/about-congenital-heart-defects

American Heart Association. "Common Types of Heart Defects." n.d. Accessed on September 19, 2018. http://www.heart.org/en/health-topics/congenital-heart-defects/about-congenital-heart-defects/common-types-of-heart-defects

Barallobre-Barreiro, Javier, Athanasios Didangelos, Friedrich Schoendube A., Ignat Drozdov, Xiaoke Yin, Mariana Ferna´ndez-Caggiano, Peter Willeit, et al. 2012. "Proteomics analysis of cardiac extracellular matrix remodeling in a porcine model of ischemia/reperfusion injury." Circulation 125 (6): 789-802.

Benrashid, Ehsan, Christopher C. McCoy, Linda M. Youngwirth, Jina Kim, Roberto J. Manson, James C. Otto, and Jeffrey H. Lawson. 2016. "Tissue engineered vascular grafts: Origins, development, and current strategies for clinical application." Methods 99: 13-19.

Benton, Julie A., Cole A. DeForest, Vani Vivekanandan, and Kristi S. Anseth. 2009. "Photocrosslinking of gelatin macromers to synthesize porous hydrogels that promote valvular interstitial cell function." Tissue engineering Part A 15 (11): 3221-3230.

Bond, Andrew R., Dominga Iacobazzi, Safa Abdul-Ghani, Mohammed Ghorbel, Kate Heesom, Mariangela Wilson, Christopher Gillett et al. 2018a. "Changes in contractile protein expression are linked to ventricular stiffness in infants with pulmonary hypertension or right ventricular hypertrophy due to congenital heart disease." Open Heart 5: e000716.

Bond A.R., Iacobazzi D., Abdul-Ghani S., Ghorbel M. T., Heesom K. J., George S.J., Caputo M., Suleiman M.-S., Tulloh R.M. 2018b "The cardiac proteome in patients with congenital ventricular septal defect: A comparative study between right atria and right ventricles." Journal of Proteomics doi.org/10.1016/j.jprot.2018.03.022.

Botto, Lorenzo D., Adolfo C. 2001. "Racial and temporal variations in the prevalence of heart defects." Pediatrics 107 (3): E32.

Brandley, Brian K. and Ronald L. Schnaar. 1989. "Tumor cell haptotaxis on covalently immobilized linear and exponential gradients of a cell adhesion peptide." Developmental Biology 135 (1): 74-86.

Brightman, A. O., B. P. Rajwa, J. E. Sturgis, M. E. McCallister, J. P. Robinson, and S. L. Voytik‐Harbin. 2000. "Time-lapse confocal reflection microscopy of collagen fibrillogenesis and extracellular matrix assembly in vitro." Biopolymers 54: 222–234.

Crapo, Peter M., Thomas W. Gilbert, and Stephen F. Badylak. 2011. "An overview of tissue and whole organ decellularization processes." Biomaterials 32 (12): 3233-3243.

Castañeda, Aldo. 2005. "Congenital heart disease: A surgical-historical perspective" The Annals of Thoracic Surgery 79: S2217–2220)

Cio, Stefania Di, Thea M.L.Bøggild, JohnConnelly, Duncan S. Sutherland, and Julien E. Gautrot. 2017. "Differential integrin expression regulates cell sensing of the matrix nanoscale geometry." Acta Biomaterialia 50: 280-292.

Chen, Ruth R. and David J. Mooney. 2003. "Polymeric growth factor delivery strategies for tissue engineering." Pharmaceutical Research 20(8): 1103-1112.

Chung, Albert E. and Marian E. Durkin. 1990. "Entactin: Structure and Function." American Journal of Respiratory Cell and Molecular Biology 3: 275-282.

Dai, Wangde, Paul Gerczuk, Yuanyuan Zhang, Leona Smith, Oleg Kopyov, Gregory L. Kay, Aarne J. Jyrala, and Robert A. Kloner. 2013. "Intramyocardial injection of heart tissue-derived extracellular matrix improves postinfarction cardiac function in rats." Journal of Cardiovascular Pharmacology and Therapeutics 18(3): 270-279.

Danen, Erik H. J. n.d. "Integrins: An overview of structural and functional aspects." Madame Curie Bioscience Database [Internet]Bioscience Database [Internet]. Austin (TX): Landes Bioscience: 2000-2013. Accessed on September 28, 2018. https://www.ncbi.nlm.nih.gov/books/NBK6259/

Diagnostic and Interventional Cardiology. n.d. "FDA clears CorMatrix ECM for vascular repair." Accessed on August 19, 2018. https://www.dicardiology.com/product/fda-clears-cormatrix-ecm-vascular-repair

Dijkman, Petra E., Anita Driessen-Mol, Laura Frese, Simon P. Hoerstrup, and Frank P. T. Baaijens. 2012. "Decellularized homologous tissue-engineered heart valves as off-the-shelf alternatives to xeno- and homografts" Biomaterials 33 (18): 4545-4554.

Dvir, Tal, Brian P. Timko, Mark D. Brigham, Shreesh R. Naik, Sandeep S Karajanagi, Oren Levy, Hongwei Jin, Kevin K. Parker, Robert Langer, and Daniel S. Kohane. 2011. "Nanowired three-dimensional cardiac patches." Nature Nanotechnology 6: 720-725.

Fassot, Céline, Marie Briet, Philippe Rostagno, Pascal Barbry, Claudine Perret, Dominique Laude, Pierre Boutouyrie, et al. 2008. "Accelerated arterial stiffening and gene expression profile of the aorta in patients with coronary artery disease." Journal of Hypertension 26: 747–757.

Frantz, Christian, Kathleen M. Stewart, and Valerie M. Weaver. 2010. "The extracellular matrix at a glance." Journal of Cell Science 123 (24): 4195-4200.

Fujimoto, Kazuro L., Jianjun Guan, Hideki Oshima, Tetsuro Sakai, and William R. Wagner. 2007. "In vivo evaluation of a porous, elastic, biodegradable patch for reconstructive cardiac procedures." The Annals of Thoracic Surgery 83: 648-654.

Gaetani, Roberto, Peter A. Doevendans, Corina H. G. Metz, Jacqueline Alblas, Elisa Messina, Alessandro Giacomello, and Joost P. G. Sluijter. 2012. "Cardiac tissue engineering using tissue printing technology and human cardiac progenitor cells. Biomaterials 33: 1782e1790.

Geiger, Benjamin, Alexander Bershadsky, Roumen Pankov, and Kenneth M.Yamada. 2001. "Transmembrane extracellular matrix-cytoskeleton crosstalk." Nature Reviews Molecular Cell Biology 2(11): 793-805.

Godier-Furnémont, Amandine F. G., Timothy P. Martens, Michael S. Koeckert, Leo Wan, Jonathan Parks, Kotaro Arai, Geping Zhang et al. 2011. "Composite scaffold provides a cell delivery platform for cardiovascular repair." PNAS 108: 7974-7979.

Gordon, Marion K. and Rita A. Hahn. 2010. "Collagens." Cell and Tissue Research 339(1): 247–257.

Greenberg, Charles S., Paul J. Birckbichler, and Robert H. Rice. 1991. "Transglutaminases: multifunctional cross-linking enzymes that stabilize tissues." The FASEB Journal 5(15): 3071-3077.

Gubbiotti, Maria A., Thomas Neill, and Renato V. Iozzo. 2017. "A current view of perlecan in physiology and pathology: A mosaic of functions." Matrix Biology 57-58: 285–298.

Hamill, Kevin J., Kristina Kligys, Susan B. Hopkinson, and Jonathan C. R. Jones. 2009. "Laminin deposition in the extracellular matrix: a complex picture emerges." Journal of Cell Science 122 (24): 4409-4417.

Hansen, Kirk C., Lauren Kiemele, Ori Maller, Jenean O'Brien, Aarthi Shankar, Jaime Fornetti, and Pepper Schedi. 2015. "An in-solution ultrasonication-assisted digestion method for improved extracellular matrix proteome coverage." Molecular & Cellular proteomics 17 (8): 1648-1657.

Hata, Hiroki, Antonia Bär, Suzanne Dorfman, Zlata Vukadinovic, Yoshiki Sawa, Axel Haverich, and Andres Hilfiker. 2010. "Engineering a novel three-dimensional

contractile myocardial patch with cell sheets and decellularised matrix." European Journal of Cardio-Thoracic Surgery 38 (4): 450–455.

Hibino, Narutoshi, Edward McGillicuddy, Goki Matsumura, MD, Yuki Ichihara, Yuji Naito, Christopher Breuer, Toshiharu Shinoka. 2010. "Late-term results of tissue-engineered vascular grafts in humans." The Journal of Thoracic and Cardiovascular Surgery 139: 431-436.

Hibino, Narutoshi, Gustavo Villalona, Nicholas Pietris, Daniel R. Duncan, Adam Schoffner, Jason D. Roh, Tai Yi et al. 2011. "Tissue-engineered vascular grafts form neovessels that arise from regeneration of the adjacent blood vessel." The FASEB Journal 25(8): 2731-2739.

Hill, Ryan C., Elizabeth Calle A., Monika Dzieciatkowska, Laura Niklason E., and Kirk C. Hansen. 2015. "Quantification of extracellular matrix proteins from a rat lung scaffold to provide a molecular readout for tissue engineering." Molecular & Cellular Proteomics 14: 961-973.

Hoerstrup, Simon P., Ian Cummings, Mario Lachat, Frederick J. Schoen, Rolf Jenni, Sebastian Leschka, Stefan Neuenschwander, Dörthe Schmidt, Anita Mol, Christina Günter, Mathias Gössi, Michele Genoni, and Gregor Zund. 2006. "Functional growth in tissue-engineered living, vascular grafts: follow-up at 100 weeks in a large animal model." Circulation 114 (Suppl I): 159-166.

Hofmann, Michael, Martin O. Schmiady, Barbara E. Burkhardt, Hitendu H. Dave, Michael Hübler, Oliver Kretschmar, and Peter K. Bode. 2017. "Congenital aortic valve repair using CorMatrix: A histologic evaluation." Xenotransplantation 24(6): e12341.

Holst, Kimberly A., Sameh M. Said, Timothy J. Nelson, Bryan C. Cannon, Joseph A. Dearani. 2017. "Current interventional and surgical management of congenital heart disease specific focus on valvular disease and cardiac arrhythmias." Circulation Research 120:1027-1044.

Hussey, George S., Jenna L. Dziki, and Stephen F. Badylak. 2018. "Extracellular matrix- based materials for regenerative medicine." Nature Reviews Materials 3: 159-173.

Irvine, Darrell J., Kerri-Ann Hue, Anne M. Mayes, and Linda G. Griffith. 2002. "Simulations of cell-surface integrin binding to nanoscale-clustered adhesion ligands." Biophysical Journal 82(1): 120-132.

Jayakrishnan, A. and Jameela, S.R. 1999. "Glutaraldehyde as a fixative in bioprostheses and drug delivery matrices." Biomaterials 17 (5): 471-484.

Johnson, Todd D., Stephen Y. Lin, and Karen L. Christman. 2011. "Tailoring material properties of a nanofibrous extracellular matrix derived hydrogel." Nanotechnology 22(49): 494015.

Johnson, Todd D., Jessica A. DeQuach, Roberto Gaetani, Jessica Ungerleider, Dean Elhag, Vishal Nigam, Atta Behfard, and Karen L. Christman. 2014. "Human versus porcine tissue sourcing for an injectable myocardial matrix hydrogel." Biomaterials Science 2: 735-744.

Johnson, Todd D., Ryan C. Hill, Monika Dzieciatkowska, Vishal Nigam, Atta Behfar, Karen L. Christman and Kirk C. 2016. Hansen "Quantification of decellularized human myocardial matrix: A comparison of six patients." Proteomics Clinical Applications 10: 75–83.

Jorge-Herrero, E., Fernández P. Turnay J., Olmo N., Calero P., García R. Freile I., and Castillo-Olivares J.L. 1999. "Influence of different chemical cross-linking treatments on the properties of bovine pericardium and collagen." Biomaterials 20(6): 539-545.

Jung, MoonSun, Megan S. Lord, Bill Cheng, J. Guy Lyons, Hatem Alkhouri, J. Margaret Hughes, Simon J. McCarthy, Renato V. Iozzo, and John M. Whitelock. 2013. "Mast cells produce novel shorter forms of perlecan that contain functional endorepellin: A role in angiogenesis and wound healing." Journal of Biological Chemistry 288: 3289–3304.

Kato, Nobuyasu, Masaaki Yamagishi, Keiichi Kanda, Takako Miyazaki, Yoshinobu Maeda, Masashi Yamanami, Taiji Watanabe, and Hitoshi Yaku. 2016. "First successful clinical application of the in vivo tissue-engineered autologous vascular graft." The Annals of Thoracic Surgery 102:1387–1390.

Kimura, Naritaka. 2018."Regenerative therapy for patients with congenital heart disease." The Keio Journal of Medicine https://doi.org/10.2302/kjm.2018-0002-IR

Kisiday J., M. Jin, B. Kurz, H. Hung, C. Semino, S. Zhang, and A. J. Grodzinsky. 2002. "Self-assembling peptide hydrogel fosters chondrocyte extracellular matrix production and cell division: Implications for cartilage tissue repair." PNAS 99 (15): 9996-10001.

Kraft, Paul, John Mills, and Edward Dratz. 2001. "Mass spectrometric analysis of cyanogen bromide fragments of integral membrane proteins at the picomole level: Application to Rhodopsin." Analytical Biochemistry 292: 76-86.

Lindsey, Merry L., Michael E. Hall, Romain Harmancey, and Yonggang Ma. 2016. "Adapting extracellular matrix proteomics for clinical studies on cardiac remodeling post-myocardial infarction." Clinical Proteomics 13: 19.

Li, Ren-Ke, Zhi-Qiang Jia, Richard D. Weisel, Donald A. G. Mickle, Angel Choi, and Terrence M. Yau. 1999. "Survival and function of bioengineered cardiac grafts." Circulation 100 (Suppl II): 63-69.

Li, Xia, Jin Zhou, Zhiqiang Liu, Jun Chen, Shuang hongLü, Hongyu Sun, Junjie Li, and Qiuxia Lin. 2014. "A PNIPAAm-based thermosensitive hydrogel containing SWCNTs for stem cell transplantation in myocardial repair." Biomaterials 35: 5679-5688.

Lodish, Harvey, Arnold Berk, Lawrence Zipursky, Paul Matsudaira, David Baltimore, and James Darnell. Molecular Cell Biology. 4th edition. New York: W. H. Freeman; 2000.

Lord, Megan S., Christine Y. Chuang, James Melrose, Michael J. Davies, Renato V. Iozzo, and John M. Whitelock. 2014. "The role of vascular-derived perlecan in modulating cell adhesion, proliferation and growth factor signaling." Matrix Biology 35: 112–122.

Lutolf, M. P. and J. A. Hubbell. 2005. "Synthetic biomaterials as instructive extracellular microenvironments for morphogenesis in tissue engineering" Nature Biotechnology 23 (1): 47-55.

Malm, T., S. Bowald, A. Bylock, Ch. Busch, and T. Saldeen. 1994. "Enlargement of the right ventricular outflow tract and the pulmonary artery with a new biodegradable patch in transannular position." European Surgical Research 26(5): 298-308.

Mann, Brenda K., Gobin, Andrea S., Annabel T. Tsai, Rachael H. Schmedlen, and Jennifer L. West. 2001. "Smooth muscle cell growth in photopolymerized hydrogels with cell adhesive and proteolytically degradable domains: synthetic ECM analogs for tissue engineering." Biomaterials 22(22): 3045-3051.

Matsumura, Goki, Naotaka Nitta, Shojiro Matsuda, Yuki Sakamoto, Noriko Isayama, Kenji Yamazaki, and Yoshito Ikada. 2012. "Long-term results of cell-free biodegradable scaffolds for in situ tissue-engineering vasculature: In a canine inferior vena cava model." PLoS One. 7(4): e35760.

MedlinePlus. n.d. "Congenital heart defect - corrective surgery." Accessed on October 5, 2018. https://medlineplus.gov/ency/article/002948.htm

Methe, Ketaki, Henrik Backdahl, Bengt R. Johansson, Nikhil Nayakawde, Goran Dellgren, and Suchitra Sumitran-Holgersson. 2014. "An alternative approach to decellularize whole porcine heart" BioResearch Open Access 3 (6): 327-338.

Mouw, Janna K., Guanqing Ou, and Valerie M. Weaver. 2014. "Extracellular matrix assembly: a multiscale deconstruction." Nature Reviews Molecular Cell Biology 15 (12): 771-785.

Naba, Alexandra, Karl R. Clauser, Sebastian Hoersch, Hui Liu, Steven A. Carr, and Richard O. Hynes. 2012. "The matrisome: In silico definition and in vivo characterization by proteomics of normal and tumor extracellular matrices." Molecular & Cellular Proteomics 11: 10.1074/mcp.M111.014647, 1–18.

Navaei, Ali, Harpinder Saini, Wayne Christenson, Ryan Tanner Sullivan, Robert Ros, and Mehdi Nikkhah. 2016. "Gold nanorod-incorporated gelatin-based conductive hydrogels for engineering cardiac tissue constructs." Acta Biomaterialia 41: 133–146.

Navaei, Ali, Nathan Moore, Ryan T. Sullivan, Danh Truong, Raymond Q. Migrino, and Mehdi Nikkhah. "Electrically conductive hydrogel-based micro-topographies for the development of organized cardiac tissues." RSC Advances 7: 3302-3312.

Nelson, Jennifer S., Amer Heider, Ming-Sing Si, and Richard G. Ohye. 2016. "Evaluation of Explanted CorMatrix intracardiac patches in children with congenital heart disease." The Annals of Thoracic Surgery 102:1329–1335.

Nichol, Jason W., Sandeep Koshy, Hojae Bae, Chang Mo Hwang, Seda Yamanlar, and Ali Khademhosseini. 2010. "Cell-laden microengineered gelatin methacrylate hydrogels" Biomaterials 31 (21): 5536-5544.

Nikoobakht, Babak, and Mostafa A. El-Sayed. 2003. "Preparation and growth mechanism of gold nanorods (NRs) using seed-mediated growth method." Chemistry of Materials 15 (10): 1957-1962.

Nucleus Medical Media. 2015. "Congenital heart anomalies in the newborn" [Digital image]. Retrieved from http://catalog.nucleusmedicalmedia.com/congenital-heart-anomalies-in-the-newborn/view-item?ItemID=1593

Oberpenning, Frank, Jun Meng, James J. Yoo, and Anthony Atala. 1999. "De novo reconstitution of a functional mammalian urinary bladder by tissue engineering." Nature biotechnology 17: 149-155.

Oberwallner, Barbara, Andreja Brodarac, Yeong-Hoon Choi, Tomo Saric, Petra Anić, Lars Morawietz, and Christof Stamm. 2014. "Preparation of cardiac extracellular matrix scaffolds by decellularization of human myocardium." Journal of Biomedical Materials Research Part A 102A: 3263–3272.

Ott, Harald C., Thomas S. Matthiesen, Saik-Kia Goh, Lauren D. Black, Stefan M. Kren, Theoden I. Netoff and Doris A. Taylor. 2008. "Perfusion-decellularized matrix: Using nature's platform to engineer a bioartificial heart." Nature Medicine 14: 213-221.

Oyamada, Masahito, Hisakazu Kimura, Yumiko Oyamada, Atsushi Miyamoto, Hideyo Ohshika, and Michio Mori. 1994. "The expression, phosphorylation, and localization

of connexin 43 and gap-junctional intercellular communication during the establishment of a synchronized contraction of cultured neonatal rat cardiac myocytes." Experimental Cell Research 212 (2): 351-358.

Ozawa, Tsukasa, Donald A.G. Mickle, Richard D. Weisel, Nobuya Koyama, Harvey Wong, Sumiko Ozawa, and Ren-Ke Li. 2002a. "Histologic changes of nonbiodegradable and biodegradable biomaterials used to repair right ventricular heart defects in rats." The Journal of Thoracic and Cardiovascular Surgery 124(6): 1157-64.

Ozawa, Tsukasa, Donald A. G. Mickle, Richard D. Weisel, Nobuya Koyama, Sumiko Ozawa, and Ren-Ke Li. 2002b. "Optimal Biomaterial for Creation of Autologous Cardiac Grafts." Circulation 106[suppl I]:I-176-I-182.

Patterson, Joseph T, Thomas Gilliland, Mark W. Maxfield, Spencer Church, Yuji Naito, Toshiharu Shinoka, and Christopher K. Breuer. 2012. "Tissue-engineered vascular grafts for use in the treatment of congenital heart disease: from the bench to the clinic and back again." Regenerative Medicine 7(3): 409-419.

Pok, Seokwon, Flavia Vitale, Shannon L. Eichmann, Omar M. Benavides, Matteo Pasquali, and Jeffrey G. Jacot. 2014. "Biocompatible carbon nanotube–chitosan scaffold matching the electrical conductivity of the heart." ACS Nano 8 (10): 9822-9832.

Quarti, Andrea, Stefania Nardone, Massimo Colaneri, Gaetano Santoro, and Marco Pozzi. 2011. "Preliminary experience in the use of an extracellular matrix to repair congenital heart diseases." Interactive Cardio Vascular and Thoracic Surgery 13: 569-572.

Roh, Jason D., Rajendra Sawh-Martinez, Matthew P. Brennan, Steven M. Jay, Lesley Devine, Deepak A. Rao, Tai Yi, et al. 2010. "Tissue-engineered vascular grafts transform into mature blood vessels via an inflammation-mediated process of vascular remodeling." Proceedings of the National Academy of Sciences of the United States of America 107(10): 4669-4574.

Romano, Nicole, Debanti Sengupta, Cindy Chung, and Sarah C. Heilshorn. 2011. "Protein-engineered biomaterials: Nanoscale mimics of the extracellular matrix." Biochimica et Biophysica Acta 1810(3): 339–349.

Rosario-Quinones, Frances, Margret S. Magid, Jen Yau, Amit Pawale, and Khanh Nguyen. 2015. “Tissue reaction to porcine intestinal submucosa (CorMatrix) implants in pediatric cardiac patients: A single-center experience.” Annals of Thoracic Surgery 99:1373–1377.

Saini, Harpinder, Ali Navaei, Alison Van Putten, and Mehdi Nikkhah. 2015. "3D cardiac microtissues encapsulated with the co-culture of cardiomyocytes and cardiac fibroblasts." Advanced Healthcare Materials 4 (13): 1961-1971.

Sakai, Tetsuro, Ren-Ke Li, Richard D. Weisel, Donald A.G. Mickle, Eung T. Joong Kim, Zhi-Qian Jia, and Terrence M. Yau. 2001. “The fate of a tissue-engineered cardiac graft in the right ventricular outflow tract of the rat.” The Journal of Thoracic and Cardiovascular Surgery 121: 932-942.

Scholl, Frank G., Mark M. Boucek, Kak-Chen Chan, Lilliam Valdes-Cruz, and Richard Perryman. 2010. “Preliminary experience with cardiac reconstruction using decellularized porcine extracellular matrix scaffold: Human applications in congenital heart disease.” World Journal for Pediatric and Congenital Heart Surgery I (I) 132-136.

Schulte, Jason B., Agneta Simionescu, and Dan T. Simionescu. 2013. “The acellular myocardial flap: A novel extracellular matrix scaffold enriched with patent microvascular networks and biocompatible cell niches.” Tissue Engineering: Part C 19 (7): 518-529.

Schwartz, Martin Alexander. 2010. “Integrins and extracellular matrix in mechanotransduction.” Cold Spring Harbor Perspectives in Biology 2(12):a005066.

Seif-Naraghi, Sonya B., Jennifer M. Singelyn, Michael A. Salvatore, Kent G. Osborn, Jean J. Wang, Unatti Sampat, Oi Ling Kwan et al. 2013. “Safety and efficacy of an injectable extracellular matrix hydrogel for treating myocardial infarction.” Science Translational Medicine 5 (173): 173ra25.

Serban Monica A. and Glenn D. Prestwich. 2008. “Modular extracellular matrices: solutions for the puzzle” Methods 45(1): 93–98.

Shimizu, Tatsuya, Hidekazu Sekine, Joseph Yang, Yuki Isoi, Masayuki Yamato, Akihiko Kikuchi, Eiji Kobayashi, and Teruo Okano. 2006. "Polysurgery of cell sheet grafts overcomes diffusion limits to produce thick, vascularized myocardial tissues." The FASEB Journal 20(6): 708-710.

Shin'oka, Toshiharu, Goki Matsumura, Narutoshi Hibino, Yuji Naito, Manabu Watanabe, Takeshi Konuma, Takahiko Sakamoto, Masayoshi Nagatsu, and Hiromi Kurosawa. 2005. "Midterm clinical result of tissue-engineered vascular autografts seeded with autologous bone marrow cells." The Journal of Thoracic and Cardiovascular Surgery 129(6): 1330-1338.

Singelyn, Jennifer M., Jessica A. DeQuach, Sonya B. Seif-Naraghi, Robert B. Littlefield, Pamela J. Schup-Magoffin, and Karen L. Christman. 2009. "Naturally derived myocardial matrix as an injectable scaffold for cardiac tissue engineering." Biomaterials 30: 5409–5416.

Singelyn, Jennifer M., Priya Sundaramurthy, Todd D. Johnson, Pamela J. Schup-Magoffin, Diane P. Hu, Denver M. Faulk et al. 2012. "Catheter-deliverable hydrogel derived from decellularized ventricular extracellular matrix increases endogenous cardiomyocytes and preserves cardiac function post-myocardial infarction." Journal of the American College of Cardiology 59 (8): 751-763.

Sugiura, Tadahisa, Narutoshi Hibino, Christopher K. Breuer, and Toshiharu Shinoka. 2016. "Tissue-engineered cardiac patch seeded with human induced pluripotent stem cell derived cardiomyocytes promoted the regeneration of host cardiomyocytes in a rat model." Journal of Cardiothoracic Surgery 11:163

Stock, Ulrich A., Takahiko Sakamoto, Shinichi Hatsuoka, David P. Martin, Mitsugi Nagashima, Adrian M. Moran, Marsha A. Moses, Philipe N. Khalil, Frederick J. Schoen, Joseph P. Vacanti, and John E. Mayer Jr. 2000. "Patch augmentation of the pulmonary artery with bioabsorbable polymers and autologous cell seeding." The Journal of Thoracic and Cardiovascular Surgery 120: 1158-1168.

Suna, Gonca, Wojciech Wojakowski, Marc Lynch, Javier Barallobre-Barreiro, Xiaoke Yin, Ursula Mayr, Ferheen Baig, et al. 2018. "Extracellular matrix proteomics reveals interplay of aggrecan and aggrecanases in vascular remodeling of stented coronary arteries." Circulation 137 (2):166-183.

Sundararaghavan, Harini G., Gary A. Monteiro, Norman A. Lapin, Yves J. Chabal, Jennifer R. Miksan, and David I. Shreiber. 2008. "Genipin‐induced changes in collagen gels: Correlation of mechanical properties to fluorescence." The Journal of Biomedical Materials Research 87A: 308–320.

Tanaka, Akiko, Keigo Kawaji, Amit R. Patel, Yasuhiko Tabata, Martin C. Burke, Mahesh P. Gupta, and Takeyoshi Ota. 2015. "In situ constructive myocardial remodeling of extracellular matrix patch enhanced with controlled growth factor release." The Journal of Thoracic and Cardiovascular Surgery 150:1280-90.

Tee, Richard, Zerina Lokmic, Wayne A. Morrison, and Rodney J. Dilley. 2010. "Strategies for cardiac tissue engineering." ANZ Journal of Surgery 80: 683-693.

Villarreal, Francisco J. and Noel N Kim. 1998. "Regulation of myocardial extracellular matrix components by mechanical and chemical growth factors." Cardiovascular Pathology 7 (3): 145-151.

Vit O., Man P., Kadek A., Hausner J., Sklenar J., Harant K., Novak P., Scigelova M., Woffendin G., and Petrak J. 2016. "Large-scale identification of membrane proteins based on analysis of trypsin-protected transmembrane segments." Journal of Proteomics 149: 15-22.

Wainwright, John M., Caitlin A. Czajka, Urvi B. Patel, Donald O. Freytes, Kimimasa Tobita, Thomas W. Gilbert, and Stephen F. Badylak. 2010. "Preparation of cardiac extracellular matrix from an intact porcine heart." Tissue Engineering Part C Methods 16 (3): 525-532.

Wainwright, John M., Ryotaro Hashizume, Kazuro L. Fujimoto, Nathaniel T. Remlinger, Colin Pesyna, William R. Wagner, Kimimasa Tobita, Thomas W. Gilbert, and Stephen F. Badylak. 2012. "Right ventricular outflow tract repair with a cardiac biologic scaffold." Cells Tissues Organs 195: 159-170.

Wassenaar, Jean W, Rebecca L. Braden, Kent G. Osborn, and Karen L. Christman. 2016a. "Modulating in vivo degradation rate of injectable extracellular matrix hydrogels" Jounal of Materials Chemistry B-Materials for Biology and Medicine 4(16): 2794–2802.

Wassenaar, Jean W, Roberto Gaetani, Julian J. Garcia, Rebecca L. Braden, Colin G. Luo, Diane Huang, Anthony N. DeMaria, Jeffrey H. Omens, and Karen L. Christman. 2016b. "Evidence for mechanisms underlying the functional benefits of a myocardial matrix hydrogel for post-MI treatment." Journal of the American College of Cardiology 67 (9):1074-1086.

Williams, C., K.P. Quinn, I. Georgakoudi, and L.D. Black III. 2014. "Young developmental age cardiac extracellular matrix promotes the expansion of neonatal cardiomyocytes in vitro." Acta Biomaterialia 10: 194–204.

Williams, Corin, Erica Budina, Whitney L. Stoppel, Kelly E. Sullivan, Sirisha Emani, Sitaram M. Emani, and Lauren D. Black III. 2015. "Cardiac extracellular matrix–fibrin hybrid scaffolds with tunable properties for cardiovascular tissue engineering." Acta Biomaterialia 14: 84-95.

Witt, Russell G., Gary Raff, Jeff Van Gundy, Melissa Rodgers-Ohlau, and Ming-Sing Si 2013. "Short-term experience of porcine small intestinal submucosa patches in paediatric cardiovascular surgery." European Journal of Cardio-Thoracic Surgery 44: 72-76.

Xia, Yu, Haifa Hong, Lincai Ye, Yanlin Wang, Huiwen Chen, and Jinfen Liu. 2013. "Label-free quantitative proteomic analysis of right ventricular remodeling in infant Tetralogy of Fallot patients." Journal of Proteomics 84: 78-91.

You, Jin-Oh, Marjan Rafat, George J. C. Ye, and Debra T. Auguste. 2011. "Nanoengineering the heart: conductive scaffolds enhance connexin 43 expression." Nano Letters 11: 3643–3648.

Yue, Beatrice. 2014. "Biology of the extracellular matrix: An overview." Journal of Glaucoma: S20-S23.

Zaidi, Abbas Haider,Meena Nathan, Sitaram Emani, Christopher Baird, Pedro J. del Nido, Kimberlee Gauvreau, Marian Harris, Stephen P. Sanders, and Robert F. Padera. 2014. "Preliminary experience with porcine intestinal submucosa (CorMatrix) for valve reconstruction in congenital heart disease: Histologic evaluation of explanted valves." The Journal of Thoracic and Cardiovascular Surgery 148: 2216-2215.

Zhang, Yuanyuan, Yujiang He, Shantaram Bharadwaj, Nevin Hammam, Kristen Carnagey, Regina Myers, Anthony Atala, and Mark Van Dyke. 2009. "Tissue-specific extracellular matrix coatings for the promotion of cell proliferation and maintenance of cell phenotype." Biomaterials 30: 4021-4028.

Zheng, Chen-Xi, Bing‐Dong Sui, Cheng-Hu Hu, Xin-Yu Qiu, Pan Zhao, and Yan Jin. 2018. "Reconstruction of structure and function in tissue engineering of solid organs: Toward simulation of natural development based on decellularization." Journal of Tissue Engineering and Regenerative Medicine: 1–16.

Zimmermann, Wolfram-Hubertus and Robert Cesnjevar. 2009. "Cardiac Tissue Engineering: Implications for Pediatric Heart Surgery." Pediatric Cardiology 30:716–723.

Zisch, Andreas H., Matthias P. Lutolf, Martin Ehrbar, George P. Raeber, Simone C. Rizzi, Neil Davies, Hugo Schmkel, et al. 2003. "Cell-demanded release of VEGF from synthetic, biointeractive cell-ingrowth matrices for vascularized tissue growth." The FASEB Journal 15: 2260-2.

Zoeller, Jason J., Angela McQuillan, John Whitelock, Shiu-Ying Ho, and Renato V. Iozzo 2008. "A central function for perlecan in skeletal muscle and cardiovascular development." Journal of Cell Biology 181:381–394. Alberts B, Johnson A, Lewis J, et al. Molecular Biology of the Cell. 4th edition. New York: Garland Science; 2002. Integrins. Available from: https://www.ncbi.nlm.nih.gov/books/NBK26867/

APPENDIX A

COPYRIGHTS AND PERMISSIONS

Figure 1

License Number	4445110068837
License date	Oct 09, 2018
Licensed Content Publisher	Elsevier
Licensed Content Publication	Current Opinion in Solid State & Materials Science
Licensed Content Title	Controlling stem cell behavior with decellularized extracellular matrix scaffolds
Licensed Content Author	Gillie Agmon,Karen L. Christman
Licensed Content Date	Aug 1, 2016
Licensed Content Volume	20
Licensed Content Issue	4
Licensed Content Pages	9
Start Page	193
End Page	201
Type of Use	Reuse in a thesis/dissertation
Intended publisher of new work	Other
Portion	Figures/tables/illustrations
Number of figures/tables/illustrations	1
Format	Both print and electronic
Are you the author of this Elsevier article?	No
Will you be translating?	No
Original figure numbers figure	1
Title of your thesis/dissertation	Development of pediatric patient-derived extracellular matrix-incorporated gelatin-based hydrogels for cardiac tissue engineering
Publisher of new work	Arizona State University
Author of new work	Dr. Mehdi Nikkhah
Expected completion date	Oct 2018
Estimated size (number of pages)	1
Publisher Tax ID	98-0397604
Total	0.00 USD

Figure 2

Invoice Date	October 10, 2018
Invoice Number	3707-01472
Terms	30 Days
PO Number	(not specified)
Nucleus Job #	3707
Job Name	Medical Image Education License -exh5892
Client#	155329
Client Name	Ms. Yuka Sugamura
Firm Name	Arizona State University
Payment made	10/10/2018
Notes	- Order #N-3707-1539202507, Yuka Sugamura, Authorization Number: 051519
Number	1
Each	($20.00)
Subtotal	($20.00)
Content License	10/10/2018
Notes	exh5892 Congenital Heart Anomalies in the Newborn - Journal/Magazine - Master - 10/15/2018 to 04/15/2019
Number	1
Each	$20.00
Subtotal	$20.00
Balance Due	$0.00

Figure 3

License Number	4445110612149
License date	Oct 09, 2018
Licensed Content Publisher	John Wiley and Sons
Licensed Content Publication	Journal of Tissue Engineering and Regenerative Medicine
Licensed Content Title	Reconstruction of structure and function in tissue engineering of solid organs: Toward simulation of natural development based on decellularization
Licensed Content Author	Chen - Xi Zheng, Bing - Dong Sui, Cheng - Hu Hu, et al
Licensed Content Date	May 15, 2018
Licensed Content Volume	12
Licensed Content Issue	6
Licensed Content Pages	16
Type of use	Dissertation/Thesis
Requestor type	University/Academic
Format	Print and electronic
Portion	Figure/table
Number of figures/tables	2
Original Wiley figure/table number(s)	Figure 2
Will you be translating?	No
Title of your thesis/ dissertation	Development of pediatric patient-derived extracellular matrix-incorporated gelatin-based hydrogels for cardiac tissue engineering
Expected completion date	Oct 2018
Expected size (number of pages)	1
Publisher Tax ID	EU826007151
Total	0.00 USD

Figure 12

License Number	4442510833827
License date	Oct 05, 2018
Licensed content publisher	American Society for Biochemistry and Molecular Biology
Licensed content title	Molecular
Licensed content date	Jan 1, 2002
Type of Use	Thesis/Dissertation
Requestor type	Academic institution
Format	Print, Electronic
Portion	chart/graph/table/figure
Number of charts/graphs/tables/figures	1
The requesting person/organization is:	Arizona State University
Title or numeric reference of the portion(s)	Quantification of extracellular matrix proteins from a rat lung scaffold to provide a molecular readout for tissue engineering Figure 1
Title of the article or chapter the portion is from	N/A
Editor of portion(s)	N/A
Author of portion(s)	Ryan C. Hill, Elizabeth A. Calle, Monika Dzieciatkowska, Laura E. Niklason and Kirk C. Hansen
Volume of serial or monograph.	14
Issue, if republishing an article from a serial	4
Page range of the portion	965
Publication date of portion	February 8, 2015
Rights for	Main product
Duration of use	Current edition and up to 5 years
Creation of copies for the disabled	no
With minor editing privileges	no
For distribution to	Worldwide
In the following language(s)	Original language of publication
With incidental promotional use	no
The lifetime unit quantity of new product	Up to 499
Title	Development of Pediatric Patient-Derived Extracellular Matrix-Incorporated Gelatin-Based Hydrogels for Cardiac Tissue Engineering
Instructor name	Dr. Mehdi Nikkhah
Institution name	Arizona State University
Expected presentation date	Oct 2018
Billing Type	Invoice
Total (may include CCC user fee)	0.00 USD